

European Centre  
for Medium Range  
Weather Forecasts

Normal Modes of a Barotropic Version  
of the ECMWF Gridpoint Model

Internal Report 12  
Research Dept.

July 77

Centre Européen pour les Prévisions Météorologiques  
à Moyen Terme

Europäisches Zentrum Für Mittelfristige Wettervorhersagen

NORMAL MODES OF A BAROTROPIC  
VERSION OF THE E.C.M.W.F.  
GRIDPOINT MODEL

---

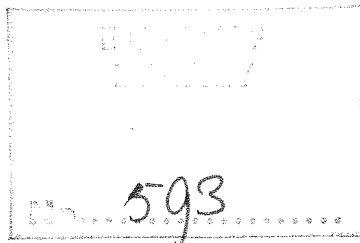
by

C. Temperton

European Centre for Medium Range Weather Forecasts, Bracknell

Internal Report No. 12

RESEARCH DEPARTMENT



July 1977

N O T E:

This paper has not been published and should be regarded as an Internal Report from ECMWF Research Department.

Permission to quote from it should be obtained from the Deputy Director, Head of Research, at ECMWF.

## 1. Introduction

Despite a considerable amount of research over the past twenty years, one of the outstanding problems of numerical weather prediction is still that of initialization, i.e. providing a primitive equation model with initial conditions such that the forecast integration is not contaminated by spurious high-frequency gravity-wave oscillations. There is disagreement, even between groups involved in operational forecasting, on the impact of initialization on the accuracy of the subsequent forecast, and on the best means of achieving the required balance. For an overview of the initialization problem, and some of the suggested solutions, see BENGTTSSON (1975).

It is envisaged that a research program will be carried out at ECMWF to try to resolve some of the problems by systematically comparing the results of various initialization procedures, first using a simple barotropic model but concentrating later on a full-scale multi-level operational prediction model.

Particular attention is likely to be focussed on a relatively new approach to the problem, based on the application of the normal modes of the linearized model equations. FLATTERY (1970) based his analysis scheme (now used at NMC) on the Hough functions, which are the normal modes of the linearized shallow-water equations on a rotating sphere, expressed in continuous form. DICKINSON and WILLIAMSON (1972, henceforth referred to as D & W) proposed an initialization scheme based directly on the normal modes of the finite-difference equations of a gridpoint model; some experimental results for a shallow-water equation model were reported by WILLIAMSON (1976). The normal modes of a multi-level general circulation model have also been computed and used as a diagnostic tool (WILLIAMSON and DICKINSON, 1976). The normal mode analysis also provides information on the linear stability of finite-difference schemes, with particular reference to means of improving the stability of a regular latitude-longitude grid formulation on the sphere, e.g. by Fourier filtering the higher zonal wavenumbers near the pole (WILLIAMSON, 1976a).

The results reported by WILLIAMSON (1976b) demonstrated that, although the amplitudes of gravity-wave oscillations were considerably reduced by means of a normal mode initialization procedure, substantial oscillations were still present as a result of the nonlinearity of the forecast model. Recent research has extended the normal mode approach to initialization to include forcing by the nonlinear terms (BAER, 1977; MACHENHAUER, 1977).

In this paper, the basis of the normal mode initialization procedure is briefly explained. The derivation of the normal modes of a shallow-water equation model (using the finite-difference formulation of the ECMWF gridpoint forecast model)

is outlined, and the results compared with those of D & W. The effects of Fourier filtering procedures are also studied.

## 2. Why normal modes ?

A numerical weather prediction model consists essentially of a large set of coupled ordinary differential equations. The dependent variables may be gridpoint values of temperature, wind components, etc.; or coefficients of prescribed basis functions, as in spectral models. If all the dependent variables are combined into a single vector  $\tilde{x}$ , then the system of equations can be written as

$$\frac{d\tilde{x}}{dt} = L\tilde{x} + M\tilde{x} \quad (1)$$

where the matrix  $L$  represents the linear terms (i.e.,  $L$  is independent of  $\tilde{x}$ ), and the matrix  $M$  represents the nonlinear terms ( $M$  depends on  $\tilde{x}$ ). In order to solve the system (1) we require a set of initial conditions at time  $t_0$ , say  $\tilde{x}(t_0) = \tilde{x}_0$ .

In deriving the normal modes of the model, we linearize Eq.(1), for convenience about a state of rest. From the point of view of the initialization scheme, this is similar to the assumptions made in deriving the geostrophic relationship or the linear balance equation (indeed, for a periodic  $f$ -plane the outcome of the normal mode analysis is precisely the geostrophic relationship). So, instead of Eq.(1), we consider the simpler system

$$\frac{d\tilde{x}}{dt} = L\tilde{x} \quad (2)$$

In effect we are assuming that  $M\tilde{x}$  is in some sense small compared with  $L\tilde{x}$ , and that solutions of Eq.(2) will for some time approximate solutions of Eq.(1), given the same set of initial conditions.

From the theory of matrices we know that there exist matrices  $E, \Lambda$  such that  $L = E\Lambda E^{-1}$ , where  $\Lambda$  is diagonal and contains the eigenvalues of  $L$ , while the columns of  $E$  are the eigenvectors of  $L$ . In fact it will turn out that  $L$  is real and antisymmetric, so that  $E^{-1} = E^T$  (the transpose of  $E$ ), and the eigenvalues of  $L$  are all purely imaginary; thus it is convenient to write  $\Lambda = \text{diag} (i\lambda_1, i\lambda_2, \dots)$ . Substituting for  $L$  and writing

$$\tilde{y} = E^{-1}\tilde{x},$$

Eq. (2) is transformed into the form

$$\frac{d\tilde{y}}{dt} = \Lambda\tilde{y} \quad (3)$$

Since  $\Lambda$  is diagonal, Eq.(3) is simply a set of equations of the form

$$\frac{dy_1}{dt} = i\lambda_1 y_1$$

$$\frac{dy_2}{dt} = i\lambda_2 y_2$$

⋮  
⋮  
⋮

to which the solution is clearly

$$y_1(t) = y_1(t_0) \exp(i\lambda_1(t-t_0))$$

$$y_2(t) = y_2(t_0) \exp(i\lambda_2(t-t_0))$$

⋮  
⋮  
⋮

and hence

$$\tilde{x}(t) = \tilde{E}y(t) = E \begin{bmatrix} y_1(t_0)\exp(i\lambda_1(t-t_0)) \\ y_2(t_0)\exp(i\lambda_2(t-t_0)) \\ \vdots \\ \vdots \end{bmatrix} \quad (4)$$

Denoting the columns of  $E$  (i.e., the eigenvectors of  $L$ ) by  $\{\tilde{\Psi}_j\}$ , we can rewrite Eq.(4) as

$$\tilde{x}(t) = \sum_j y_j(t_0) \tilde{\Psi}_j \exp(i\lambda_j(t-t_0)) \quad (5)$$

Eq.(5) shows that the solution  $\tilde{x}(t)$  consists of a sum of oscillations of frequency  $\lambda_j$ , each associated with a normal mode  $\tilde{\Psi}_j$  of the system. The constants  $y_j(t_0)$  are determined from the initial conditions by the relationship  $\tilde{x}(t_0) = E^{-1}\tilde{x}(t_0)$ , and are referred to as the normal mode coefficients.

The idea of normal mode initialization is to define  $\hat{y}(t_0)$  by setting  $y_j(t_0) = 0$  for those normal modes corresponding to gravity-wave solutions, and to replace  $\tilde{x}(t_0)$  by  $\hat{x}(t_0) = \hat{E}\hat{y}(t_0)$ , thus removing the gravity-wave oscillations from the solution given by Eq.(5).

### 3. Finite-difference equations of the model

To set up the finite-difference equations of the model, we first impose a grid over the surface of the earth, defined by intersections of lines of latitude ( $\theta$ ) and longitude ( $\lambda$ ). We define gridlengths  $\Delta\lambda = 2\pi/N$  and  $\Delta\theta = \pi/2M$ , so that there are  $N$  gridlengths around each line of latitude, and  $M$  gridlengths

between equator and pole. The gridpoint (i,j) has coordinates (iΔλ, jΔθ).

For a barotropic model, we have three different variables: u (zonal wind component), v (meridional wind component) and φ (geopotential height). For the finite-difference formulation of the ECMWF gridpoint model, there are distributed over the grid as shown in Fig. 1, with φ defined at points (i,j), u at (i+½, j), and v at (i, j+½).

In setting down the equations for the model, we use the following conventional finite-difference operators:

$$\bar{A}^x = \frac{1}{2} [A(x+\frac{1}{2}\Delta x) + A(x-\frac{1}{2}\Delta x)]$$

$$\delta_x A = [A(x+\frac{1}{2}\Delta x) - A(x-\frac{1}{2}\Delta x)] / \Delta x$$

The equations for the multi-level gridpoint model are given in the report by BURRIDGE and HASELER (1977). For the barotropic model, the corresponding equations are:

$$\frac{\partial u}{\partial t} - \frac{1}{\cos\theta} [\bar{Z}V\cos\theta] + \frac{1}{a\cos\theta} \delta_\lambda (\phi + E) = 0 \quad (6)$$

$$\frac{\partial v}{\partial t} + [\bar{Z}U] + \frac{1}{a} \delta_\theta (\phi + E) = 0 \quad (7)$$

$$\frac{\partial \phi}{\partial t} + \frac{1}{a\cos\theta} \{\delta_\lambda U + \delta_\theta (V\cos\theta)\} = 0 \quad (8)$$

where  $Z = \frac{1}{a \cos\theta\phi} \lambda\theta \{af\cos\theta + \delta_\lambda v - \delta_\theta (u\cos\theta)\}$

$$E = \frac{1}{2} \left\{ u^2 + \frac{1}{\cos\theta} \frac{\partial}{\partial \theta} (v^2 \cos\theta) \right\}$$

$$U = \bar{\phi}^\lambda u$$

$$V = \bar{\phi}^\theta v$$

and f is the Coriolis parameter, a is the radius of the earth.

The forms of the rotation terms  $[\bar{Z}V\cos\theta]$  and  $[\bar{Z}U]$  chosen to conserve both energy and absolute potential enstrophy are given by BURRIDGE and HASELER (1977).

Linearizing the system (6) - (8) about a state of rest (u=0, v=0, φ=φ̄ everywhere), we obtain the system;

$$\frac{\partial u}{\partial t} j - \frac{1}{2 \cos \theta} \{ f_j^- \cos \theta_{j-\frac{1}{2}} \bar{v}_{j-\frac{1}{2}}^\lambda + f_j^+ \cos \theta_{j+\frac{1}{2}} \bar{v}_{j+\frac{1}{2}}^\lambda \} + \frac{1}{a \cos \theta} \delta_\lambda \phi = 0 \quad (9)$$

$$\frac{\partial v}{\partial t} j + \frac{1}{2} \{ f_{j+1}^+ \bar{u}_{j+1}^\lambda + f_j^- \bar{u}_j^\lambda \} + \frac{1}{a} \delta_\theta \phi = 0 \quad (10)$$

$$\frac{\partial \phi}{\partial t} + \frac{\phi}{a \cos \theta} \{ \delta_\lambda u + \delta_\theta (v \cos \theta) \} = 0 \quad (11)$$

where

$$f_j^+ = (\cos \frac{1}{2} \Delta \theta)^{-1} \{ \frac{2}{3} f_{j+\frac{1}{2}} + \frac{1}{3} f_{j-\frac{1}{2}} \}$$

and

$$f_j^- = (\cos \frac{1}{2} \Delta \theta)^{-1} \{ \frac{1}{3} f_{j+\frac{1}{2}} + \frac{2}{3} f_{j-\frac{1}{2}} \}$$

It will be convenient in the linearized system of equations to regard  $\phi$  as the deviation from the mean value  $\bar{\phi}$ .

As in the multi-level nonlinear model, we have to take some special measures near the poles. There is a ring of v-points  $\frac{1}{2} \Delta \theta$  from the pole, and the equations at these points require values of  $f^+$  and  $u$  at the pole itself. Using arguments analogous to those of BURRIDGE and HASELER (1977), it can be shown that at the north pole:

$$f_M^+ = (\cos \frac{1}{2} \Delta \theta)^{-1} f_{M-\frac{1}{2}}$$

$$\text{and } [u]_M = 0 \quad (12)$$

where  $[ ]$  denotes a zonal average, and

$$\begin{aligned} & (\Delta \lambda)^{-1} (u_{i+\frac{1}{2}, M} - u_{i-\frac{1}{2}, M}) - (\frac{1}{2} \Delta \theta)^{-1} v_{i, M-\frac{1}{2}} \cos \theta_{M-\frac{1}{2}} \\ & = -(\frac{1}{2} \Delta \theta)^{-1} [v]_{M-\frac{1}{2}} \cos \theta_{M-\frac{1}{2}} \end{aligned} \quad (13)$$

and similarly at the south pole. Eqs. (12) and (13) are sufficient to determine the "computational" values of  $u_M$  required by the prediction equations for  $v_{M-\frac{1}{2}}$ .

The equation for  $\phi$  at the north pole becomes:

$$\frac{\partial \phi}{\partial t} M - \frac{4 \phi}{a \Delta \theta} [v]_{M-\frac{1}{2}} = 0 \quad (14)$$

#### 4. Determination of the normal modes

In principle we now have sufficient information to compute the matrix  $L$  of Eq.(1) and to determine its eigenvalues and



eigenvectors. However, even with the modest resolution  $\Delta\lambda = \Delta\theta = 3.75^\circ$  ( $M = 24$ ,  $N = 96$ ), a global barotropic model has 13634 degrees of freedom, and the matrices  $L$  and  $E$  would each occupy nearly  $2 \times 10^8$  memory locations. (Of course, most of the entries of  $L$  are zero). Fortunately, a great amount of simplification is possible.

First, we note that the solutions of Eqs. (9) - (11) can be divided into two separate classes depending on symmetry about the equator. "Symmetric" solutions have  $u(i,-j)=u(i,j)$ ;  $v(i,-j) = -v(i,j)$ ;  $\phi(i,-j) = \phi(i,j)$ , while "antisymmetric" solutions have  $u(i,-j) = -u(i,j)$ ;  $v(i,-j) = v(i,j)$ ;  $\phi(i,-j) = -\phi(i,j)$ . From now on we consider the two classes of solutions separately.

Instead of considering the equations in the form of the system (9) - (11), we can separate the longitudinal dependence of the variables by Fourier transforming the system. This is equivalent to defining

$$\phi(\lambda, \theta, t) = \sum_{k=0}^{N-1} \hat{\phi}_k(\theta, t) \exp(ik\lambda)$$

and similarly for  $u$  and  $v$ . The coefficients  $\hat{\phi}_k$  are in general complex, but the reality of the fields implies that  $\hat{\phi}_{N-k}$  must be the complex conjugate of  $\hat{\phi}_k$ ; hence we need consider only wavenumbers  $0 \leq k \leq N/2$ .

We also assume that the solutions will be periodic in time, i.e. proportional to  $\exp(i\nu t)$  for some frequency  $\nu$ , and that a leapfrog scheme is used for differencing in time.

The system (9) - (11) is transformed into the following:

$$i\nu \hat{u}_j - \frac{1}{\cos\theta_j} \frac{c(k)}{2} \{f_j^- \cos\theta_{j-\frac{1}{2}} v_{j-\frac{1}{2}} + f_j^+ \cos\theta_{j+\frac{1}{2}} \hat{v}_{j+\frac{1}{2}}\} + \frac{ik'}{a \cos\theta_j} \hat{\phi}_j = 0 \quad (15)$$

$$i\nu \hat{v}_{j+\frac{1}{2}} + \frac{c(k)}{2} \{f_{j+1}^+ \hat{u}_{j+1} + f_j^- \hat{u}_j\} + \frac{1}{a\Delta\theta} \{\hat{\phi}_{j+1} - \hat{\phi}_j\} = 0 \quad (16)$$

$$i\nu \hat{\phi}_j + \frac{\phi}{a \cos\theta_j} \{ik' \hat{u}_j + \frac{1}{\Delta\theta} [\hat{v}_{j+\frac{1}{2}} \cos\theta_{j+\frac{1}{2}} - \hat{v}_{j-\frac{1}{2}} \cos\theta_{j-\frac{1}{2}}]\} = 0 \quad (17)$$

where  $\nu' = [\sin(\nu\Delta t)]/\Delta t$   
 $c(k) = \cos(\frac{1}{2}k\Delta\lambda)$   
 $k' = [\sin(\frac{1}{2}k\Delta\lambda)]/(\frac{1}{2}\Delta\lambda)$



and the wavenumber index  $k$  has for convenience been dropped from the coefficients  $\hat{u}$ ,  $\hat{v}$  and  $\hat{\phi}$ .

Next define the following new variables:

$$u_j^* = \hat{u}_j$$

$$v_{j+\frac{1}{2}}^* = -i\hat{v}_{j+\frac{1}{2}}$$

$$\phi_j^* = \hat{\phi}_j/c, \text{ where } c = \hat{\phi}_j^{\frac{1}{2}}$$

and  $\sigma_j = \cos\theta_j$ .

Eqs. (15) - (17) then become:

$$\begin{aligned} \sigma_j v_j^* u_j^* - \frac{1}{2}c(k)\{f_j^- \sigma_{j-\frac{1}{2}} v_{j-\frac{1}{2}}^* + f_j^+ \sigma_{j+\frac{1}{2}} v_{j+\frac{1}{2}}^*\} \\ + \frac{k'c}{a} \phi_j^* = 0 \end{aligned} \quad (18)$$

$$\begin{aligned} \sigma_{j+\frac{1}{2}} v_{j+\frac{1}{2}}^* - \frac{1}{2}c(k)\{f_{j+1}^+ \sigma_{j+\frac{1}{2}} u_{j+1}^* + f_j^- \sigma_{j+\frac{1}{2}} u_j^*\} \\ - \frac{c\sigma_{j+\frac{1}{2}}}{a\Delta\theta} \{\phi_{j+1}^* - \phi_j^*\} = 0 \end{aligned} \quad (19)$$

$$\sigma_j v_j^* \phi_j^* + \frac{c}{a}\{k' u_j^* + \frac{\sigma_{j+\frac{1}{2}}}{\Delta\theta} v_{j+\frac{1}{2}}^* - \frac{\sigma_{j-\frac{1}{2}}}{\Delta\theta} v_{j-\frac{1}{2}}^*\} = 0 \quad (20)$$

As before, there are special cases near the poles.

Eq. (12) becomes:

$$u_M^* = 0 \quad \text{for } k = 0$$

and Eq. (13) becomes:

$$u_M^* = \alpha_k v_{M-\frac{1}{2}}^* \quad \text{for } k \neq 0,$$

where  $\alpha_k = 2 \cos\theta_{M-\frac{1}{2}}/k'\Delta\theta$ .

Hence for  $j = M-1$ , Eq. (19) becomes:

$$\begin{aligned} \sigma_{M-\frac{1}{2}} v_{M-\frac{1}{2}}^* - \frac{1}{2}c(k)\{f_M^+ \sigma_{M-\frac{1}{2}} \alpha_k v_{M-\frac{1}{2}}^* + f_{M-1}^- \sigma_{M-\frac{1}{2}} u_{M-1}^*\} \\ - \frac{c\sigma_{M-\frac{1}{2}}}{a\Delta\theta} \{\phi_M^* - \phi_{M-1}^*\} = 0 \end{aligned} \quad (21)$$

Note that  $\phi_M^* = 0$  for  $k \neq 0$ ; for  $k = 0$ , we have from Eq.(14):

$$\frac{1}{4} \sigma_{M-\frac{1}{2}} v_{M-\frac{1}{2}}^* - \frac{c\sigma_{M-\frac{1}{2}}}{a\Delta\theta} v_{M-\frac{1}{2}}^* = 0 \quad (22)$$

At the equator ( $j=0$ ), the form of the equations depends on whether we are considering symmetric or antisymmetric modes. For the symmetric modes, Eqs.(18)-(20) become:

$$\frac{1}{2}\sigma_0 v' u_0^* - \frac{1}{2}c(k)f_0^+ \sigma_{\frac{1}{2}} v_{\frac{1}{2}}^* + \frac{k'c}{2a} \phi_0^* = 0 \quad (23)$$

$$\begin{aligned} \sigma_{\frac{1}{2}} v' v_{\frac{1}{2}}^* - \frac{1}{2}c(k) \{f_1^+ \sigma_{\frac{1}{2}} u_1^* + f_0^- \sigma_{\frac{1}{2}} u_0^*\} \\ - \frac{c\sigma_{\frac{1}{2}}}{a\Delta\theta} \{\phi_1^* - \phi_0^*\} = 0 \end{aligned} \quad (24)$$

$$\frac{1}{2}\sigma_0 v' \phi_0^* + \frac{c}{a} \left\{ \frac{1}{2}k' u_0^* + \frac{\sigma_{j+\frac{1}{2}}}{\Delta\theta} v_{\frac{1}{2}}^* \right\} = 0 \quad (25)$$

While for the antisymmetric modes we have:

$$\begin{aligned} u_0^* &= 0 \\ \sigma_{\frac{1}{2}} v' v_{\frac{1}{2}}^* - \frac{1}{2}c(k) \{f_1^+ \sigma_{\frac{1}{2}} u_1^*\} - \frac{c\sigma_{\frac{1}{2}}}{a\Delta\theta} \phi_1^* &= 0 \\ \phi_0^* &= 0 \end{aligned} \quad (26)$$

For each wavenumber  $k$  ( $0 \leq k \leq N/2$ ), and for the symmetric and antisymmetric modes separately, Eqs. (18)-(26) determine an eigensystem, the eigenvalues of which are the frequencies  $v'$ . To write down the system compactly, define

$$\tilde{Y}_j = \begin{bmatrix} u_j^* \\ v_{j+\frac{1}{2}}^* \\ \phi_j^* \end{bmatrix}$$

$$Q_j = \begin{bmatrix} \sigma_j & & \\ & \sigma_{j+\frac{1}{2}} & \\ & & \sigma_j \end{bmatrix}$$

$$A_j = \begin{bmatrix} 0 & -\frac{1}{2}c(k)f_j^- \sigma_{j-\frac{1}{2}} & \frac{k'c}{a} \\ -\frac{1}{2}c(k)f_j^- \sigma_{j-\frac{1}{2}} & 0 & \frac{c\sigma_{j-\frac{1}{2}}}{a\Delta\theta} \\ \frac{k'c}{a} & \frac{c\sigma_{j-\frac{1}{2}}}{a\Delta\theta} & 0 \end{bmatrix}$$

$$B_j = \begin{bmatrix} 0 & 0 & 0 \\ -\frac{1}{2}c(k)f_j^+ \sigma_{j+\frac{1}{2}} & 0 & \frac{-c\sigma_{j+\frac{1}{2}}}{a\Delta\theta} \\ 0 & 0 & 0 \end{bmatrix}$$

$$C_j = \begin{bmatrix} 0 & -\frac{1}{2}c(k)f_{j-1}^+ \sigma_{j-\frac{1}{2}} & 0 \\ 0 & 0 & 0 \\ 0 & \frac{-c\sigma_{j-\frac{1}{2}}}{a\Delta\theta} & 0 \end{bmatrix} = B_{j-1}^T$$

Eqs. (18)-(20) can then be written (for each j) as

$$v' Q_j \tilde{Y}_j + C_j \tilde{Y}_{j-1} + A_j \tilde{Y}_j + B_j \tilde{Y}_{j+1} = 0 \quad (27)$$

The special cases near the poles yield the following:  
For k=0 only,

$$\underline{Y}_M = [\phi_M^*]$$

$$Q_M = [\frac{1}{2}\sigma_{M-\frac{1}{2}}]$$

$$A_M = [0]$$

$B_M$  is not required

$$C_M = [0 \quad \frac{-c\sigma_{M-\frac{1}{2}}}{a\Delta\theta} \quad 0]$$

For  $k \neq 0$ ,  $\underline{Y}_M$  etc. are not required.

For  $j = M-1$ ,  $\underline{Y}_{M-1}$ ,  $Q_{M-1}$ ,  $C_{M-1}$  are as normal, while  $A_{M-1}$  contains an extra term  $-\frac{1}{2}c(k)f_M^+\sigma_{M-\frac{1}{2}}\alpha_k$  in the central (2,2) position; and  $B_{M-1} = C_M^T$  for  $k=0$ , otherwise  $B_{M-1}$  is not required.

At the equator ( $j=0$ ) we have for symmetric modes

$$\underline{Y}_0 = \begin{bmatrix} u_0^* \\ v_{\frac{1}{2}}^* \\ \phi_0^* \end{bmatrix}$$

$$Q_0 = \begin{bmatrix} \frac{1}{2}\sigma_0 & & \\ & \sigma_{\frac{1}{2}} & \\ & & \frac{1}{2}\sigma_0 \end{bmatrix}$$

$$A_0 = \begin{bmatrix} 0 & \frac{1}{2}c(k)f_0^+\sigma_{\frac{1}{2}} & \frac{1}{2}\frac{k'c}{a} \\ \frac{1}{2}c(k)f_0^+\sigma_{\frac{1}{2}} & 0 & \frac{c\sigma_{\frac{1}{2}}}{a\Delta\theta} \\ \frac{1}{2}\frac{k'c}{a} & \frac{c\sigma_{\frac{1}{2}}}{a\Delta\theta} & 0 \end{bmatrix}$$

$B_0$  is as usual, and  $C_0$  is not required.

For antisymmetric modes,

$$\underline{Y}_0 = [v_{\frac{1}{2}}^*]$$

$$\begin{aligned} Q_0 &= [\sigma_{\frac{1}{2}}] \\ A_0 &= [0] \\ B_0 &= [-\frac{1}{2}c(k)f_1^+ \sigma_{\frac{1}{2}} \quad 0 \quad \frac{-c\sigma_{\frac{1}{2}}}{a\Delta\theta}] \end{aligned}$$

and  $C_0$  is not required. For  $j=1$ ,  $C_1 = B_0^T$ .

Now define

$$Y = \begin{bmatrix} \tilde{Y}_M \\ \tilde{Y}_{M-1} \\ \cdot \\ \cdot \\ \tilde{Y}_1 \\ \tilde{Y}_0 \end{bmatrix}$$

where the first vector  $\tilde{Y}_M$  is included only for  $k=0$ .

(The reverse ordering used here corresponds to the conventional organization of latitude lines starting at the pole and reading southwards).

Then define

$$Q = \begin{bmatrix} Q_M & & & & & \\ & Q_{M-1} & & & & \\ & & \dots & & & \\ & & & Q_1 & & \\ & & & & & Q_0 \end{bmatrix}$$
$$L = \begin{bmatrix} A_M & C_M & & & & \\ B_{M-1} & A_{M-1} & C_{M-1} & & & \\ \cdot & \cdot & \cdot & \cdot & \cdot & \cdot \\ \cdot & \cdot & \cdot & \cdot & \cdot & \cdot \\ \cdot & \cdot & \cdot & \cdot & \cdot & \cdot \\ & B_1 & A_1 & C_1 & & \\ & & B_0 & A_0 & & \end{bmatrix}$$

again including  $Q_M, A_M, C_M, B_{M-1}$  only for  $k=0$ .

Then Eq. (27) can be written as a single system:

$$\tilde{L}\tilde{Y} + v'\tilde{Q}\tilde{Y} = 0 \quad (28)$$

Since  $A_j$  is symmetric for each  $j$ , and  $B_{j-1} = C_j^T$ , the matrix  $L$  is symmetric. Also,  $Q$  is diagonal with positive entries.

Finally let

$$\begin{aligned} \hat{\tilde{Y}} &= Q^{\frac{1}{2}}\tilde{Y} \\ \hat{L} &= Q^{-\frac{1}{2}}LQ^{-\frac{1}{2}} \end{aligned}$$

and substitute in Eq. (28): the result is

$$\hat{L}\hat{\tilde{Y}} + v'\hat{\tilde{Y}} = 0 \quad (29)$$

which (apart from the sign of  $v'$ ) is in the standard form of an eigenvalue problem. Since  $L$  is real and symmetric, so is  $\hat{L}$ , and thus the eigenvalues  $v'$  are all real. Recall that the frequencies  $v$  are related to the eigenvalues  $v'$  of the system (29) by

$$v'\Delta t = \sin(v\Delta t).$$

Thus, provided that  $|v'\Delta t| \leq 1$  for all  $v'$  (the CFL linear stability criterion), all the solutions of the original system will be periodic in time, with real frequencies.

The order of the eigensystem (29), and hence the number of frequencies and corresponding normal modes, is as follows:

	Symmetric	Antisymmetric
$k=0$	$3M+1$	$3M-1$
$k \neq 0$	$3M$	$3M-2$

A program was written to set up the matrix  $L$  (given such parameters as the radius of the earth  $a$ , the rotation rate  $\Omega$ , the mean geopotential depth  $\Phi$ , and the resolution  $M, N$ ), and to find the eigenvalues and eigenvectors using the NAG routine F02ABF. Some results are presented in the next section.

## 5. Results

In order to apply the results of the normal mode analysis, we must be able to distinguish between the Rossby modes and the gravitational modes. For the continuous case, the classification is made on the basis of the behaviour of the frequencies as the equivalent depth becomes infinite (Longuet-Higgins, 1968; D & W).

As  $\phi \rightarrow \infty$ , the frequencies of the Rossby modes approach a finite value which is positive (i.e. the modes propagate westwards); the corresponding meridional velocity profile approaches the spherical harmonic  $P_{\ell+k}^k$ , with  $\ell$  zeros between the north and south poles. The number of zeros of  $v$  is thus used to index the Rossby modes.

The frequencies of the gravity modes, on the other hand, approach  $+\infty$  (for westward-travelling modes) or  $-\infty$  (for eastward-travelling modes), and the geopotential profile approaches  $P_{\ell+k}^k$ . Hence  $\ell$ , the number of zeros of  $\phi$ , is used to index the gravity modes.

For a particular value of  $k$ , the frequencies satisfy

$$\begin{aligned} v(G_{\ell}^W) &> \dots > v(G_1^W) > v(G_0^W) > \\ &v(R_0) > v(R_1) > \dots > v(R_{\ell}) > \dots > 0 > \\ &v(G_0^e) > v(G_1^e) > \dots > v(G_{\ell}^e) > \dots \end{aligned}$$

where  $R$ ,  $G^W$ ,  $G^e$  respectively denote Rossby, westward gravity and eastward gravity modes, except that for  $k=0$ , all the Rossby modes have zero frequency.

Considering now the discrete system with finite depth, we find that the Rossby and gravity wave modes are always clearly distinguishable in terms of their frequency. Appealing to considerations of symmetry, it is clear that the "symmetric" system includes the odd-indexed Rossby and even-indexed gravity-wave modes, while the "antisymmetric" system includes the even-indexed Rossby and odd-indexed gravity modes. The number of zeros does not always correspond exactly with the index  $\ell$ , partly because of the finite depth and partly due to round-off error as the modes become very close to zero over certain latitude ranges. However, the indexing can still be done in terms of the frequency ordering.

We find that the eigensystems yield the following modes:

$$\begin{aligned} \text{symmetric, } k \neq 0: & G_{2M-2}^W, \dots, G_2^W, G_0^W, R_1, R_3, \dots, R_{2M-1}, \\ & G_0^e, G_2^e, \dots, G_{2M-2}^e. \\ \text{symmetric, } k=0: & G_{2M-2}^W, \dots, G_2^W, G_0^W, R_1, R_3, \dots, R_{2M+1}, \\ & G_0^e, G_2^e, \dots, G_{2M-2}^e. \\ \text{antisymmetric, } k \neq 0: & G_{2M-3}^W, \dots, G_3^W, G_1^W, R_0, R_2, \dots, R_{2M-2}, \\ & G_1^e, G_3^e, \dots, G_{2M-3}^e. \\ \text{antisymmetric, } k=0: & G_{2M-1}^W, \dots, G_3^W, G_1^W, R_0, R_2, \dots, R_{2M-4}, \\ & G_1^e, G_3^e, \dots, G_{2M-1}^e. \end{aligned}$$



We begin our comparison with the results of D & W by considering a coarse resolution of  $\Delta\lambda = \Delta\theta = 10^\circ$  ( $M=9$ ,  $N=36$ ), with a value of  $\phi = 10^5 \text{ m}^2 \text{ s}^{-2}$  (mean equivalent depth  $D = 10 \text{ km}$ ). D & W present the frequencies  $\nu$  derived from the eigenvalues  $\gamma'$  assuming  $\Delta t = 12 \text{ min}$ . for a  $10^\circ$  grid, 6 min for a  $5^\circ$  grid, etc. Their model uses a non-staggered grid, for which the maximum stable timestep is about twice that for our staggered grid. Accordingly, the results shown here for the  $10^\circ$  ECMWF grid assume a timestep  $\Delta t = 6 \text{ min}$ .

Table 1 presents the frequencies of the Rossby modes for  $k=1$ . It is immediately obvious that the results on the ECMWF  $10^\circ$  grid resemble those of the D & W  $5^\circ$  grid, and indeed for large  $l$  they approach those of the D & W  $2\frac{1}{2}^\circ$  grid (see D & W, Table 1). In particular, they do not show the phenomenon of "bad modes", i.e. computational Rossby modes which propagate in the wrong direction. These bad modes are a consequence of aliasing in the finite-differencing scheme on a non-staggered grid, and we do not find them on our staggered grid (see Appendix).

---

Table 1 Frequencies of Rossby modes for  $D = 10$  km.,  $k=1$

$l$	ECMWF, $10^0$	D & W, $10^0$	D & W, $5^0$
0	6.11 E-05	6.07 E-05	6.12 E-05
1	1.44 E-05	1.39 E-05	1.43 E-05
2	8.64 E-06	8.08 E-06	8.60 E-06
3	5.72 E-06	5.12 E-06	5.73 E-06
4	3.98 E-06	3.32 E-06	4.02 E-06
5	2.87 E-06	2.13 E-06	2.93 E-06
6	2.14 E-06	1.27 E-06	2.20 E-06
7	1.63 E-06	5.96 E-07	1.69 E-06
8	1.27 E-06	-2.07 E-19	1.32 E-06
9	1.01 E-06	-5.96 E-07	1.04 E-06
10	8.10 E-07	-1.27 E-06	8.18 E-06
11	6.62 E-07	-2.13 E-06	6.43 E-06
12	5.52 E-07	-3.32 E-06	4.99 E-07
13	4.70 E-07	-5.12 E-06	3.77 E-07
14	4.11 E-07	-8.08 E-06	2.71 E-07
15	3.75 E-07	-1.39 E-05	1.75 E-07
16	3.13 E-07	-6.07 E-05	8.60 E-08

Table 2 Frequencies of eastward gravity modes for  $D = 10$  km.,  $k=1$

$l$	ECMWF, $10^0$	D & W, $10^0$	D & W, $5^0$
0	-5.44 E-05	-5.35 E-05	-5.38 E-05
1	-1.31 E-04	-1.28 E-04	-1.30 E-04
2	-1.87 E-04	-1.81 E-04	-1.85 E-04
3	-2.35 E-04	-2.22 E-04	-2.33 E-04
4	-2.79 E-04	-2.55 E-04	-2.78 E-04
5	-3.22 E-04	-2.78 E-04	-3.20 E-04
6	-3.63 E-04	-2.93 E-04	-3.61 E-04
7	-4.01 E-04	-3.11 E-04	-4.00 E-04
8	-4.36 E-04	-3.86 E-04	-4.34 E-04
9	-4.69 E-04	-3.86 E-04	-4.67 E-04
10	-4.98 E-04	-3.09 E-04	-4.96 E-04
11	-5.23 E-04	-2.85 E-04	-5.21 E-04
12	-5.44 E-04	-2.60 E-04	-5.42 E-04
13	-5.61 E-04	-2.30 E-04	-5.59 E-04
14	-5.72 E-04	-1.97 E-04	-5.68 E-04
15	-5.94 E-04	-1.65 E-04	-5.75 E-04
16	-5.94 E-04	-1.31 E-04	-5.91 E-04

Table 2 presents the corresponding results for the  $k=1$  eastward gravity modes. Again the frequencies of the ECMWF  $10^\circ$  grid resemble those of the D & W  $5^\circ$  grid. This time the consequence of aliasing on the non-staggered grid of D & W is that for  $l > M$  the frequencies start to decrease in magnitude instead of continuing to increase like the frequencies of the corresponding modes of the continuous equations.

Similar results were obtained for  $k=4$ , for which the frequencies are also tabulated in D & W.

For  $k=N/2$ , the Rossby modes on the ECMWF grid are stationary, since on a staggered grid the two-gridlength waves behave as if the earth were not rotating.

In order to compute the profiles of  $u$ ,  $v$  and  $\phi$  corresponding to the normal modes of the eigensystem (29), the eigenvectors must be multiplied by the diagonal matrix  $Q^{1/2}$ . Some typical results are shown in Figs. 2-5, which can be compared directly with figures presented by D & W; in all these cases the profiles obtained closely resemble those of D & W.

## 6. Fourier filtering & chopping

A familiar problem with regular latitude-longitude grids on the sphere is that the convergence of meridians towards the poles necessitates a very short timestep for computational stability. The solution usually put forward is to filter out the higher zonal wavenumbers in high latitudes (e.g. Holloway et al, 1973). There are several variants of this procedure. Williamson (1976a) discussed the effects of two of them on the normal modes of a barotropic model, and in particular derives the maximum linearly stable timestep associated with filtering out various wavenumbers.

The procedure discussed by Williamson is to filter out completely ("chop") zonal wavenumber  $k$  at latitude  $\theta$  if

$$\frac{\cos\theta}{k} < \frac{\cos\tilde{\theta}}{N/2}$$

for some critical latitude  $\tilde{\theta}$ . This procedure is applied either to all the variables, or just to the zonal pressure gradient term in the  $u$ -equation and the zonal divergence term in the  $\phi$ -equation.

Burridge & Haseler (1977) have proposed an alternative procedure for the ECMWF gridpoint model; at each timestep, the coefficient of zonal wavenumber  $k$  at latitude  $\theta$ , for the tendency  $\partial/\partial t$  of each variable, is multiplied by

Table 3 Eigenvalues for D = 10 km., 5° grid, k=7

$\ell$	unfiltered	filtered	chopped
Westward gravity modes:			
34	4.00 E-03	1.78 E-03	-
32	2.13 E-03	1.64 E-03	-
30	1.57 E-03	1.55 E-03	1.58 E-03
28	1.34 E-03	1.34 E-03	1.34 E-03
:			
2	4.74 E-04	4.74 E-04	4.74 E-04
o	3.76 E-04	3.76 E-04	3.76 E-04
Rossby modes:			
o	1.74 E-05	1.74 E-05	1.74 E-05
2	1.04 E-05	1.04 E-05	1.04 E-05
:			
14	1.66 E-06	1.66 E-06	1.65 E-06
16	1.33 E-06	1.33 E-06	1.31 E-06
18	1.08 E-06	1.08 E-06	1.05 E-06
20	8.92 E-07	8.90 E-07	8.61 E-07
22	7.50 E-07	7.47 E-07	7.18 E-07
24	6.46 E-07	6.43 E-07	6.18 E-07
26	5.75 E-07	5.73 E-07	5.54 E-07
28	5.13 E-07	5.08 E-07	4.55 E-07
30	3.77 E-07	3.61 E-07	-
32	1.77 E-07	1.13 E-07	-
34	2.26 E-08	4.71 E-09	-

$$\Lambda_k(\theta) = \frac{\cos\theta}{\cos\tilde{\theta}} \cdot \frac{1}{\sin(\frac{1}{2}k\Delta\lambda)}$$

if  $\Lambda_k(\theta) < 1$ , i.e. if

$$\frac{\cos\theta}{\sin(\frac{1}{2}k\Delta\lambda)} < \cos\tilde{\theta} \quad (30)$$

In this study we will reserve the term "filtering" for this procedure. It has also been suggested that simple Fourier chopping be applied to each variable, again based on the criterion (30). The current proposal is to set  $\tilde{\theta} = 45^\circ$ .

The Fourier filtering procedure can be incorporated into the matrices set up in Section 4 by redefining  $\sigma_j$  as

$$\sigma_j = \Lambda_k^{-1}(\theta_j) \cos\theta_j$$

if  $\Lambda_k(\theta_j) < 1$ . For Fourier chopping, the rows of the matrix corresponding to chopped variables for wavenumber  $k$  should be deleted, or (for simplicity of programming) set to zero.

For comparison with the results of Williamson (1976a), the normal modes of a barotropic version of the ECMWF gridpoint model were computed with the following parameters:

$\phi = 10^5 \text{ m}^2 \text{ s}^{-2}$  ( $D = 10 \text{ km.}$ ),  $\Delta\lambda = \Delta\theta = 5^\circ$ , using unfiltered, filtered and chopped versions. Since the maximum stable timestep  $\Delta t$  depends on the filtering procedure, Table 3 presents the eigenvalues  $\nu'$  rather than the frequencies

$\nu = (\Delta t)^{-1} \sin^{-1}(\nu' \Delta t)$ , for  $k=7$ , corresponding to waves of synoptic scale in the zonal direction. For these modes, filtering or chopping takes place beyond  $\theta = 77.5^\circ$ . As Table 3 shows, the last few modes are missing in the chopped case, while in the filtered case their frequencies are reduced; away from the limits of resolution in the meridional direction, filtering or chopping has little effect on the frequencies, especially for the gravity modes; for the Rossby modes, filtering has less effect on the frequencies than does chopping.

Williamson (1976a) presents no results for larger values of  $k$ . For completeness, we consider here the case  $k=18$ , corresponding to four-gridlength waves in the zonal direction, for which filtering or chopping is applied beyond  $\theta = 60^\circ$ . The frequencies are shown in Table 4; as expected, more modes are lost in the chopped case, and have their frequencies reduced in the filtered case. Nevertheless, at  $\ell = 18$ , corresponding to an average meridional wavelength of  $4\Delta\theta$ , the frequencies of the gravity modes are unaltered by filtering or chopping, while the frequencies of the Rossby modes are reduced by 3% by filtering, and 9% by chopping.

Turning now to the associated normal modes, Figs. 6-13 show the meridional  $\phi$  profiles for the westward gravity mode and the Rossby mode, for zonal wavenumbers  $k=7$  and  $k=18$ , and meridional indices  $\ell=6$  and  $\ell = 18$ , for the unfiltered, filtered and chopped cases. The  $\ell=6$  modes are identical to within graphical accuracy, regardless of the filtering procedure, since they contain very little energy near the poles. The  $\ell=18$  modes are slightly distorted by the filtering procedure, the effect being most noticeable for the  $k=18$ ,  $\ell=18$  Rossby mode. The chopped modes are forced to be zero beyond a certain latitude depending on  $k$ , and so their structure tends to be compressed towards the equator. Again this is most noticeable for  $k=18$ ,  $\ell=18$ ; the corresponding Rossby mode in the unfiltered case has its maximum amplitude at  $\theta=65^\circ$ , while in the chopped case the amplitude must be zero there and the maximum is forced equatorwards to  $\theta=60^\circ$ .

Table 4 Eigenvalues for  $D = 10$  km.  $5^\circ$  grid,  $k=18$ .

$\ell$	unfiltered	filtered	chopped
Westward gravity modes:			
34	9.26 E-03	1.87 E-03	-
32	4.70 E-03	1.76 E-03	-
30	3.21 E-03	1.69 E-03	-
28	2.49 E-03	1.65 E-03	-
26	2.08 E-03	1.63 E-03	-
24	1.82 E-03	1.62 E-03	1.77 E-03
22	1.64 E-03	1.61 E-03	1.62 E-03
20	1.53 E-03	1.53 E-03	1.52 E-03
:			
2	9.28 E-04	9.28 E-04	9.28 E-04
0	8.32 E-04	8.32 E-04	8.32 E-04
Rossby modes:			
0	5.92 E-06	5.92 E-06	5.92 E-06
2	4.53 E-06	4.53 E-06	4.53 E-06
:			
10	1.83 E-06	1.83 E-06	1.82 E-06
12	1.50 E-06	1.49 E-06	1.47 E-06
14	1.24 E-06	1.23 E-06	1.18 E-06
16	1.04 E-06	1.02 E-06	9.63 E-07
18	8.82 E-07	8.58 E-07	8.00 E-07
20	7.65 E-07	7.42 E-07	6.87 E-07
22	6.74 E-07	6.46 E-07	5.47 E-07
24	5.69 E-07	5.21 E-07	-
26	4.38 E-07	3.53 E-07	-
28	2.97 E-07	1.86 E-07	-
30	1.65 E-07	7.34 E-08	-
32	6.30 E-08	1.68 E-08	-
34	7.21 E-09	6.36 E-10	-

---

### 7. Calculation of normal mode coefficients

In this section we summarize the procedure for calculating the normal mode coefficients, given the fields:  $u(i+\frac{1}{2}, j)$ ,

$v(i, j+\frac{1}{2}), \phi(i, j)$  for  $0 \leq i \leq N-1, -M \leq j \leq M$ .

Step 1 Split the fields into symmetric and antisymmetric components: for example the  $u$ -field becomes

$$u_S(i+\frac{1}{2}, j) = \frac{1}{2} \{u(i+\frac{1}{2}, j) + u(i+\frac{1}{2}, -j)\}$$

$$u_A(i+\frac{1}{2}, j) = \frac{1}{2} \{u(i+\frac{1}{2}, j) - u(i+\frac{1}{2}, -j)\}$$

Henceforth we consider two separate systems  $(u_S, v_A, \phi_S)$  and  $(u_A, v_S, \phi_A)$ , and for convenience regard both systems as being defined over one hemisphere only.

Step 2 Fourier analyse the fields around lines of latitude:

$$\hat{u}(k, j) = \frac{1}{N} \omega^{-k/2} \sum_{i=0}^{N-1} u(i+\frac{1}{2}, j) \omega^{ik}$$

$$\hat{v}(k, j+\frac{1}{2}) = \frac{1}{N} \sum_{i=0}^{N-1} v(i, j+\frac{1}{2}) \omega^{ik}$$

$$\hat{\phi}(k, j) = \frac{1}{N} \sum_{i=0}^{N-1} \phi(i, j) \omega^{ik}$$

where  $\omega = \exp(2\pi i/n)$ , and for example  $u$  stands for  $u_S$  or  $u_A$ . The multiplier outside the summation sign in the  $\hat{u}$ -equation arises from the staggering of the  $u$ -points around the line of latitude. We need only consider wavenumbers  $0 \leq k \leq N/2$ .

Step 3 Scale the variables as follows:

$$u^*(k, j) = \hat{u}(k, j)$$

$$v^*(k, j+\frac{1}{2}) = -i\hat{v}(k, j+\frac{1}{2})$$

$$\phi^*(k, j) = \hat{\phi}(k, j)/c, \text{ where } c = \phi^{\frac{1}{2}}.$$

In the following steps, the vectors and matrices are as defined in Section 4, modified as necessary to include the appropriate filtering procedure.

Step 4 For each wavenumber  $k$ , form the vector  $\underline{Y}$  and multiply by the diagonal matrix  $Q^{\frac{1}{2}}$  to give  $\hat{\underline{Y}}$ .

Step 5 Multiply  $\underline{Y}$  by  $E^T$ , where  $E$  is the matrix whose columns are the eigenvectors of  $L$ . This gives the coefficients of the normal modes, ordered in the same way as the columns of  $E$ .

Linear normal mode initialization can then be performed by setting the coefficients of the gravity modes to zero and backtracking through the above procedure to recover a new set of  $u, v$  and  $\phi$  fields.



## 8. Conclusions

Computation of the normal modes of a barotropic version of the ECMWF gridpoint model shows that they closely resemble those of a model with twice the resolution on a non-staggered grid. It has also been demonstrated that the Fourier filtering and chopping procedures proposed to increase the maximum stable timestep have a significant effect only on those modes which are of such small horizontal scale that they are in any case inadequately handled by the finite-difference scheme.

References :

- Baer, F. (1977) "Adjustment of initial conditions required to suppress gravity oscillations in non-linear flows", to appear in Contributions to Atmospheric Physics, 50.
- Bengtsson, L. (1975) "4-dimensional assimilation of meteorological observations", GARP Publication No. 15.
- Burridge, D.M. and Haseler, J. (1977) "A model for medium range weather forecasts - adiabatic formulation", ECMWF Technical Report No. 4.
- Dickinson, R.E. and Williamson, D.L. (1972) "Free oscillations of a discrete stratified fluid with application to numerical weather prediction", J. Atm. Sci. 29, pp. 623-640.
- Flattery, T.W. (1970) "Spectral models for global analysis and forecasting", Proc. Sixth AWS Tech. Exchange Conf., Air Weather Service Tech. Report 242, pp.42-54.
- Holloway, J.L., Spelman, M.J. and Manabe, S. (1973) "Latitude-longitude grid suitable for numerical time integration of a global atmospheric model", Mon. Wea. Rev. 101, pp.69-78.
- Longuet-Higgins, M.S. (1968) "The eigenfunctions of Laplace's tidal equations over a sphere", Phil. Trans. Roy. Soc., London, A 262, pp. 511-607.
- Machenhauer, B. (1977) "On the dynamics of gravity oscillations in a shallow water model, with application to normal mode initialization", Contributions to Atmospheric Physics 50, pp. 253-271.

References (continued) :

- Williamson, D.L. (1976a) "Linear stability of finite-difference approximations on a uniform latitude-longitude grid with Fourier filtering", Mon. Wea. Rev. 104, pp. 31-41.
- Williamson, D.L. (1976b) "Normal mode initialization procedure applied to forecasts with the global shallow-water equations", Mon. Wea. Rev. 104, pp. 195-206.
- Williamson, D.L. and Dickinson, R.E. (1976) "Free oscillations of the NCAR Global Circulation Model", Mon. Wea. Rev. 104, pp. 1372-1391.

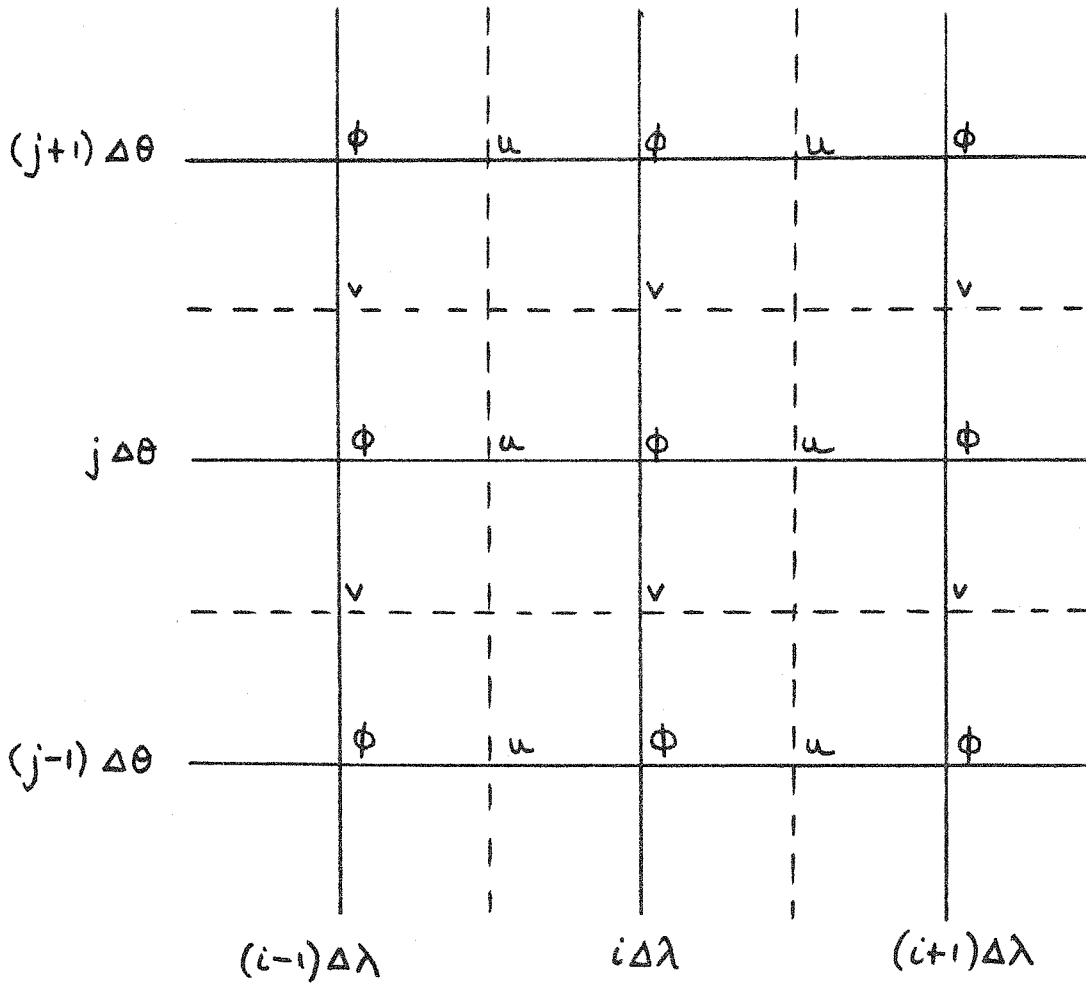


Fig. 1 Horizontal distribution of variables

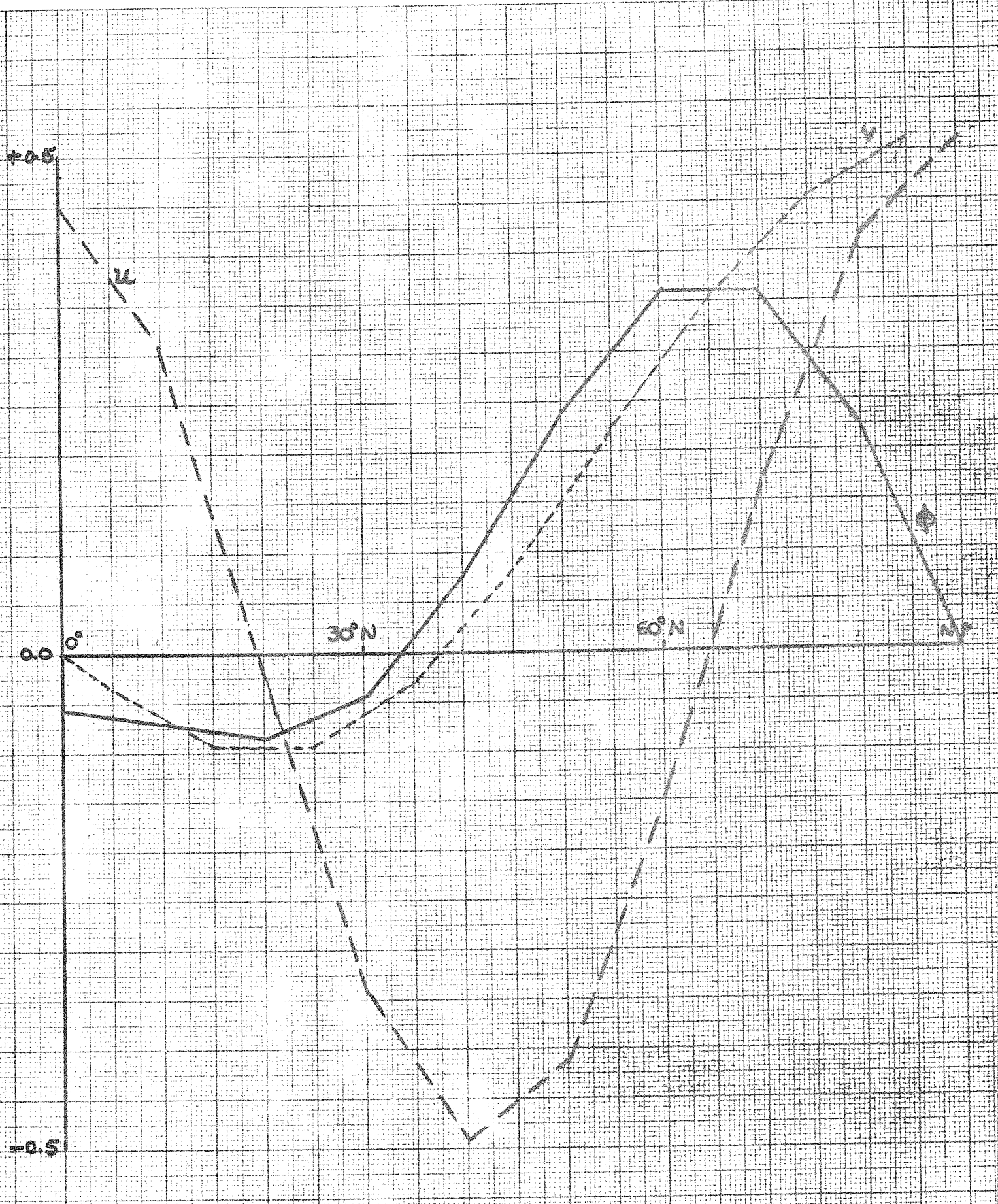


Fig. 2 Symmetric Rossby mode:  $D=10^4$  m,  $k=1$ ,  $l=3$ ;  $50MWF 10^9$  grid.  
Compare D & W Fig. 6.

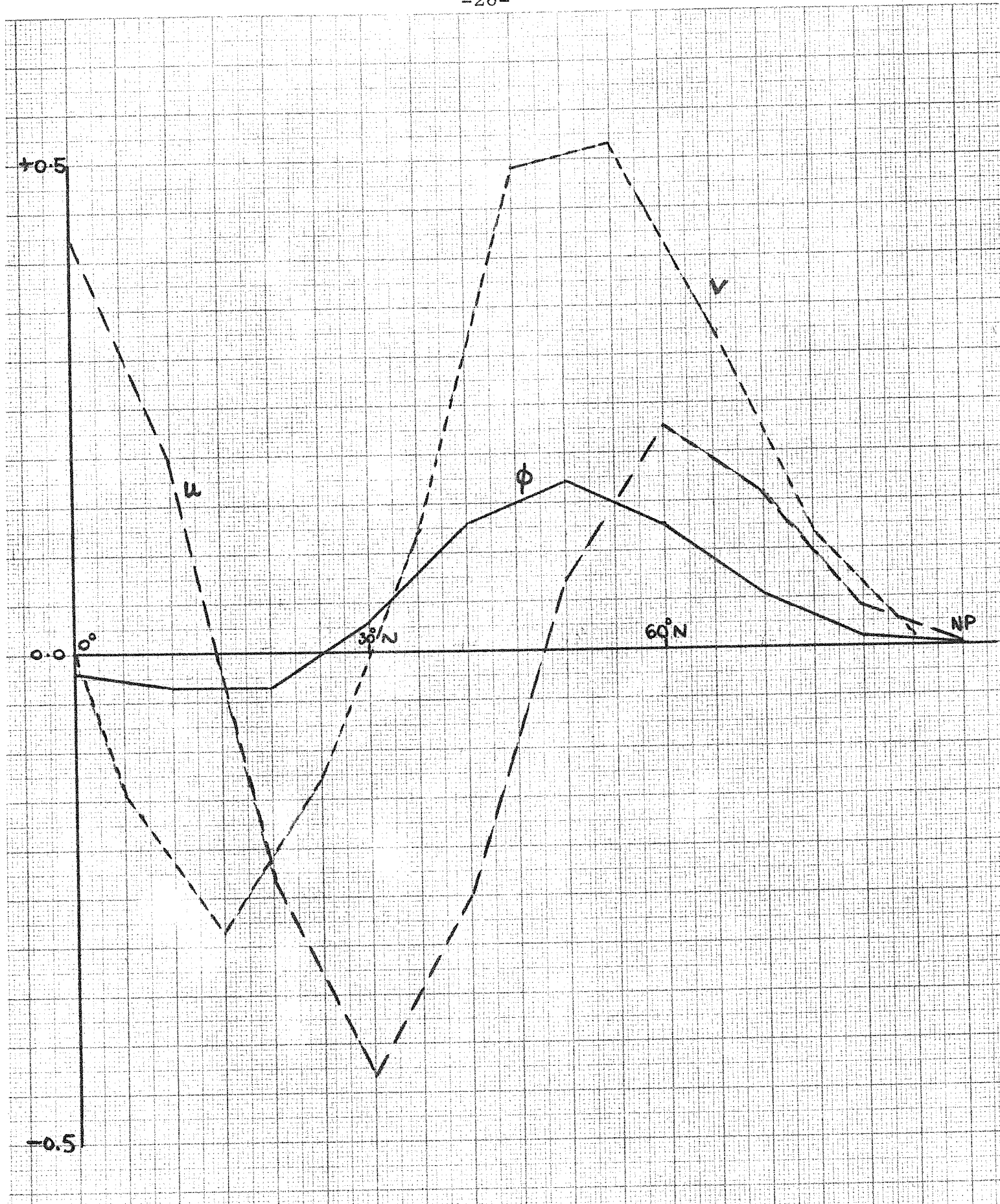


Fig. 3 Symmetric Rossby mode:  $D=10^4$  m,  $k=4$ ,  $\ell=3$ ; ECMWF  $10^\circ$  grid.  
Compare D & W Fig. 7.

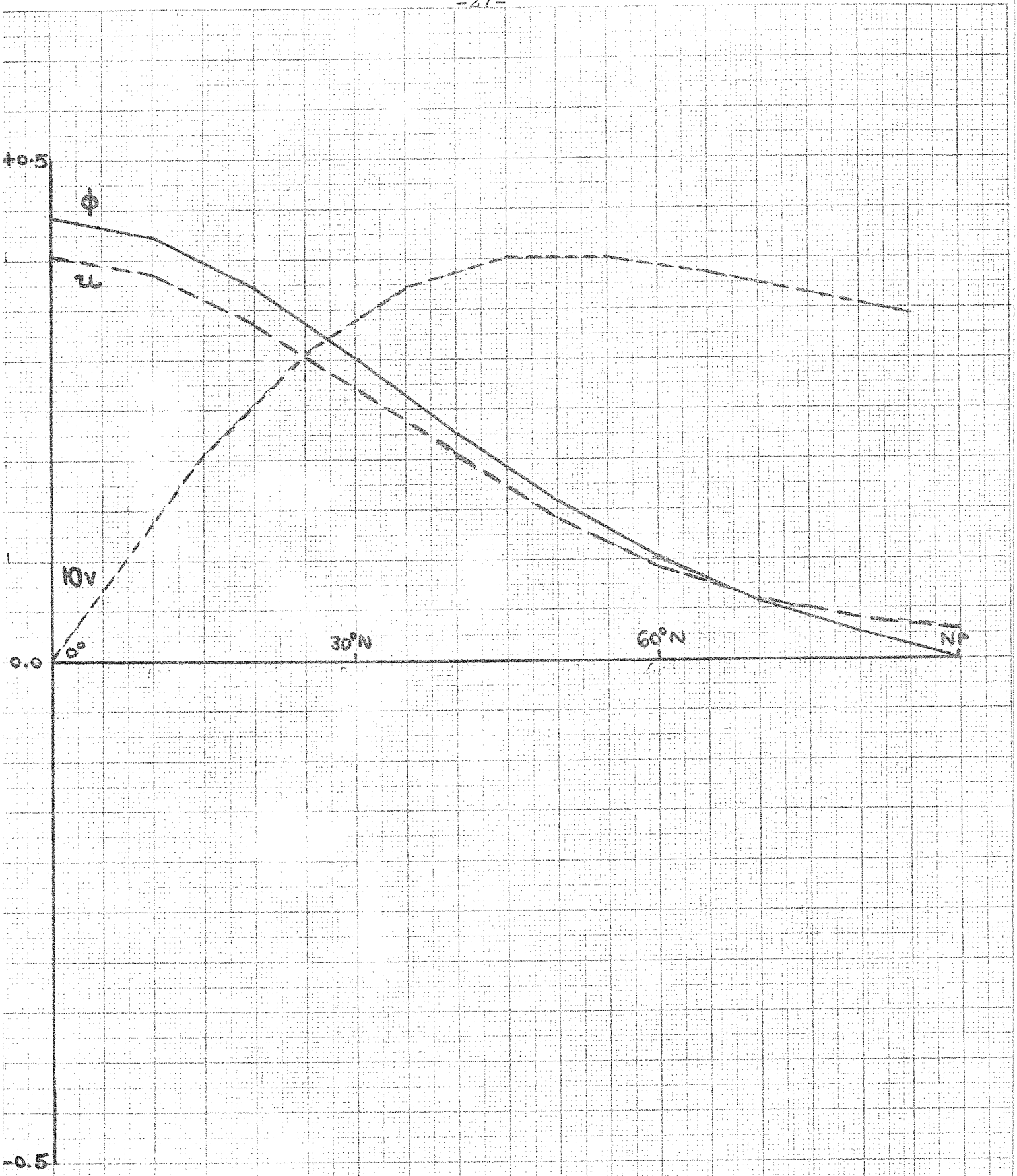


Fig. 4 Symmetric eastward gravity mode:  $D=10^4$  m,  $k=1$ ,  $l=0$ ; ECMWF  $10^\circ$  grid. Compare D & W Fig. 8.



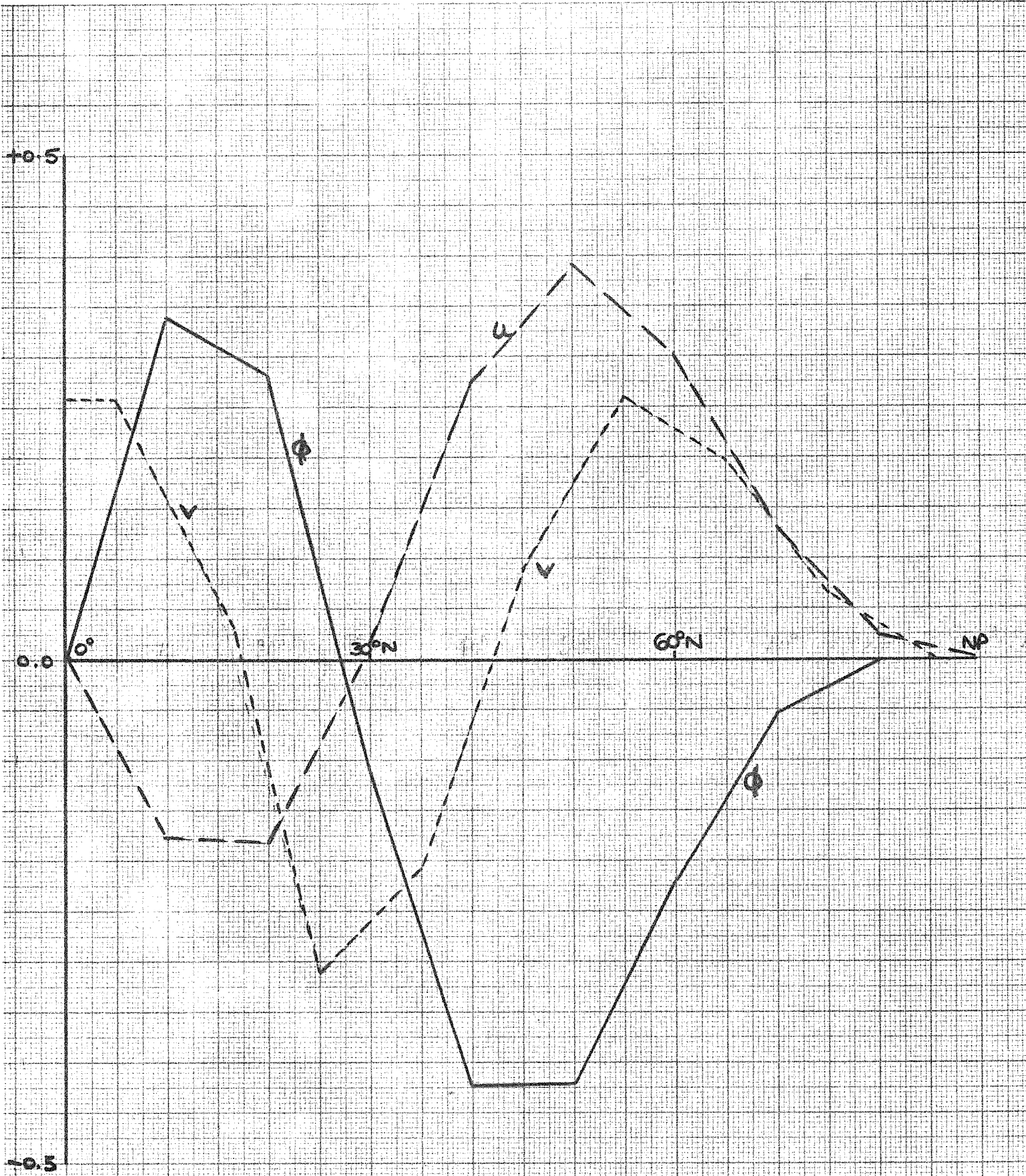


Fig. 5 Antisymmetric westward gravity mode:  $D=10^4$  m,  $k=4$ ,  $l=3$ ; ECMWF  $10^\circ$  grid.  
Compare D & W Fig. 11.

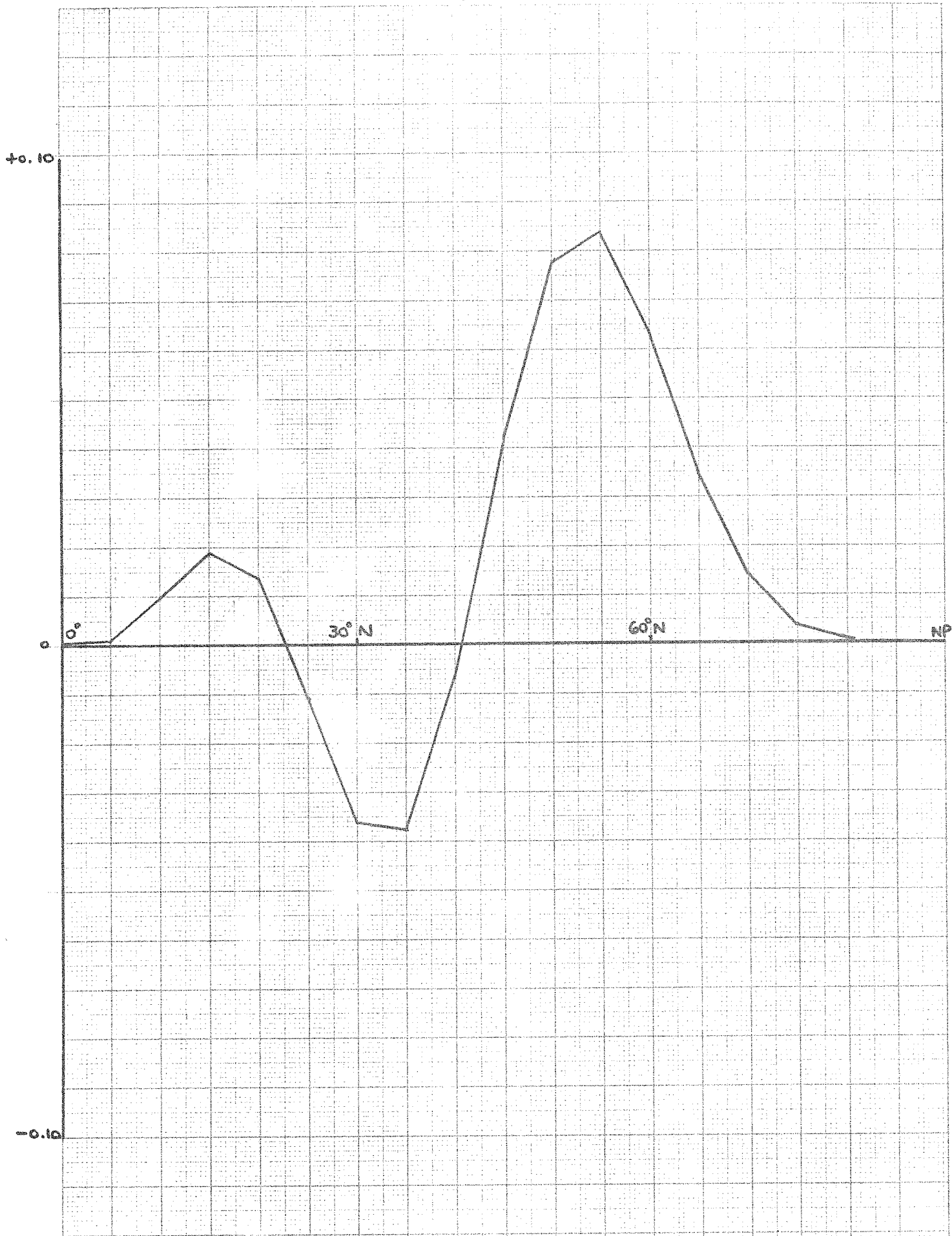


Fig. 6 Rossby mode  $\phi$  profile:  $k=7$ ,  $l=6$ . Unfiltered, filtered and chopped.

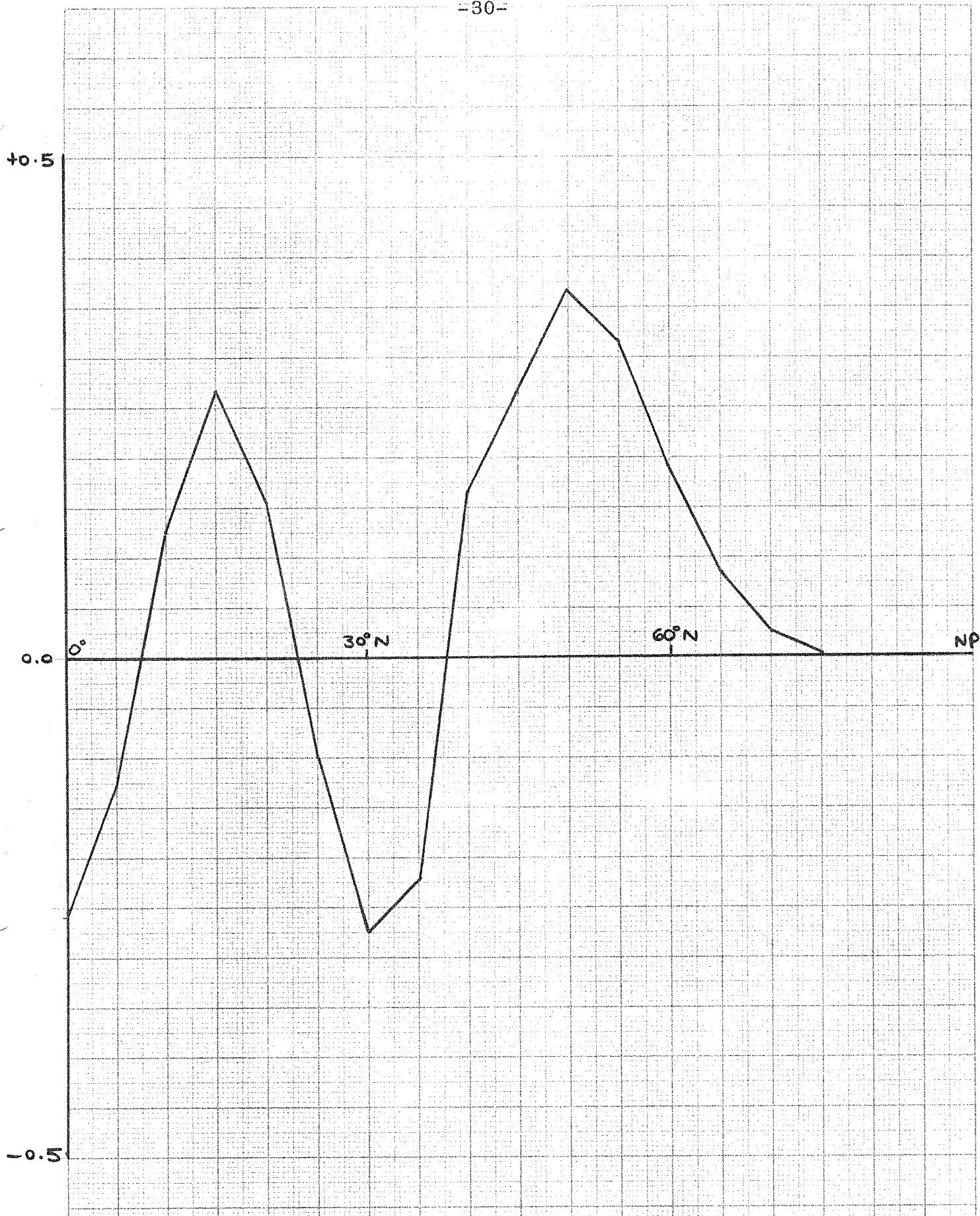


Fig. 7 Westward gravity mode  $\phi$  profile:  $k=7$ ,  $\ell=6$ . Unfiltered, filtered and chopped.

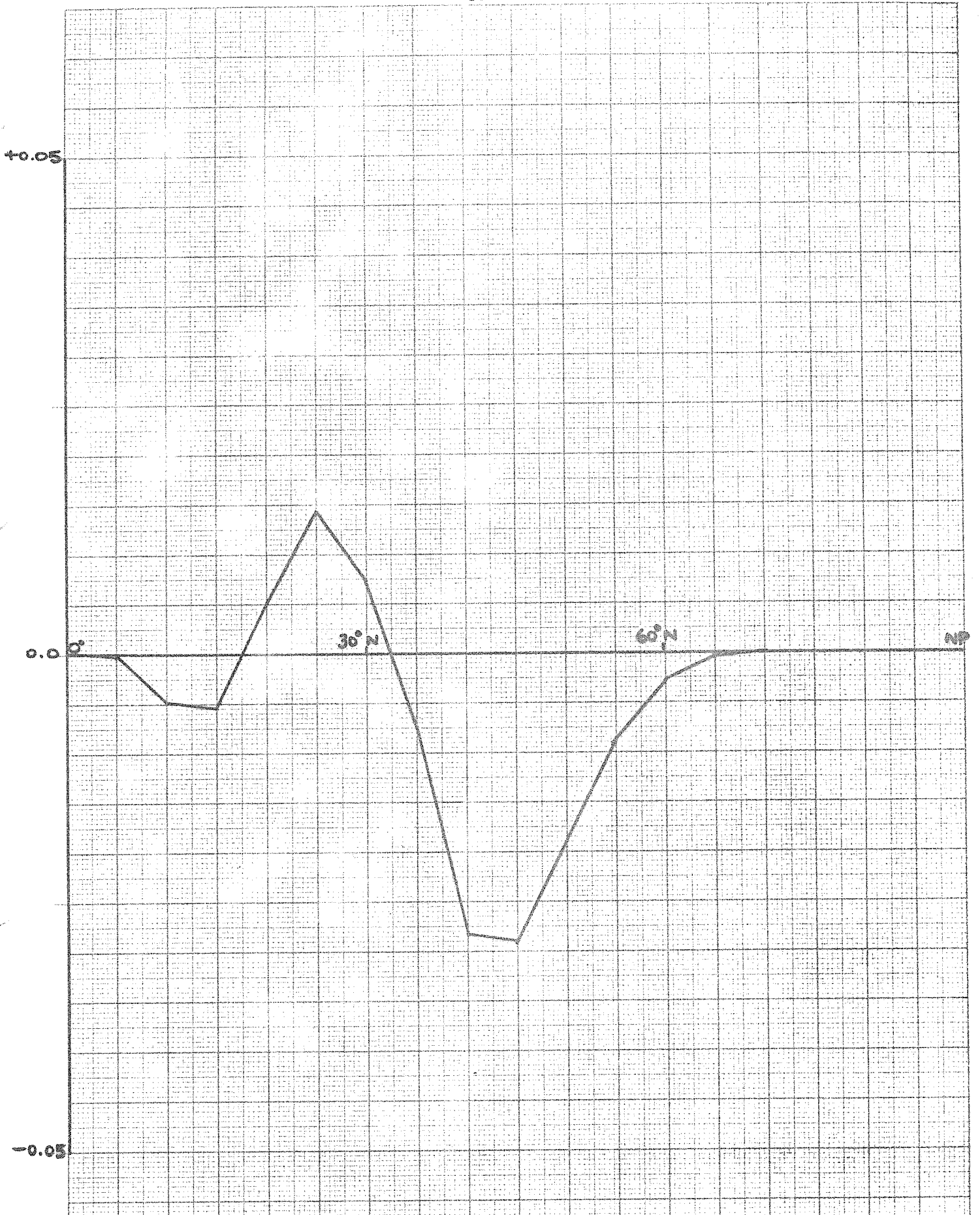


Fig. 8 Rossby mode  $\phi$  profile:  $k=18$ ,  $l=6$ . Unfiltered, filtered and chopped.

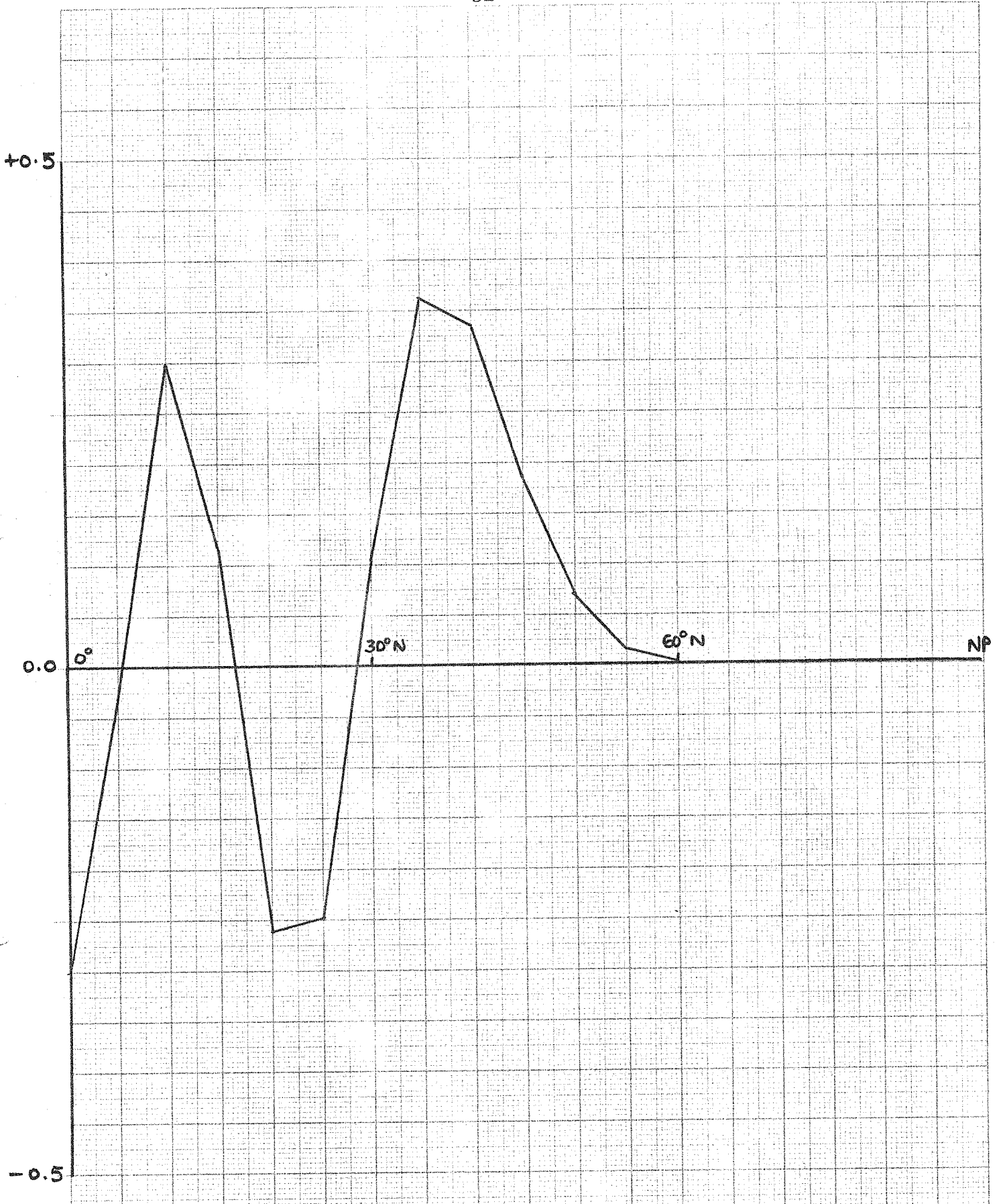


Fig. 9 Westward gravity mode  $\phi$  profile:  $k=18$ ,  $l=6$ . Unfiltered, filtered and chopped.



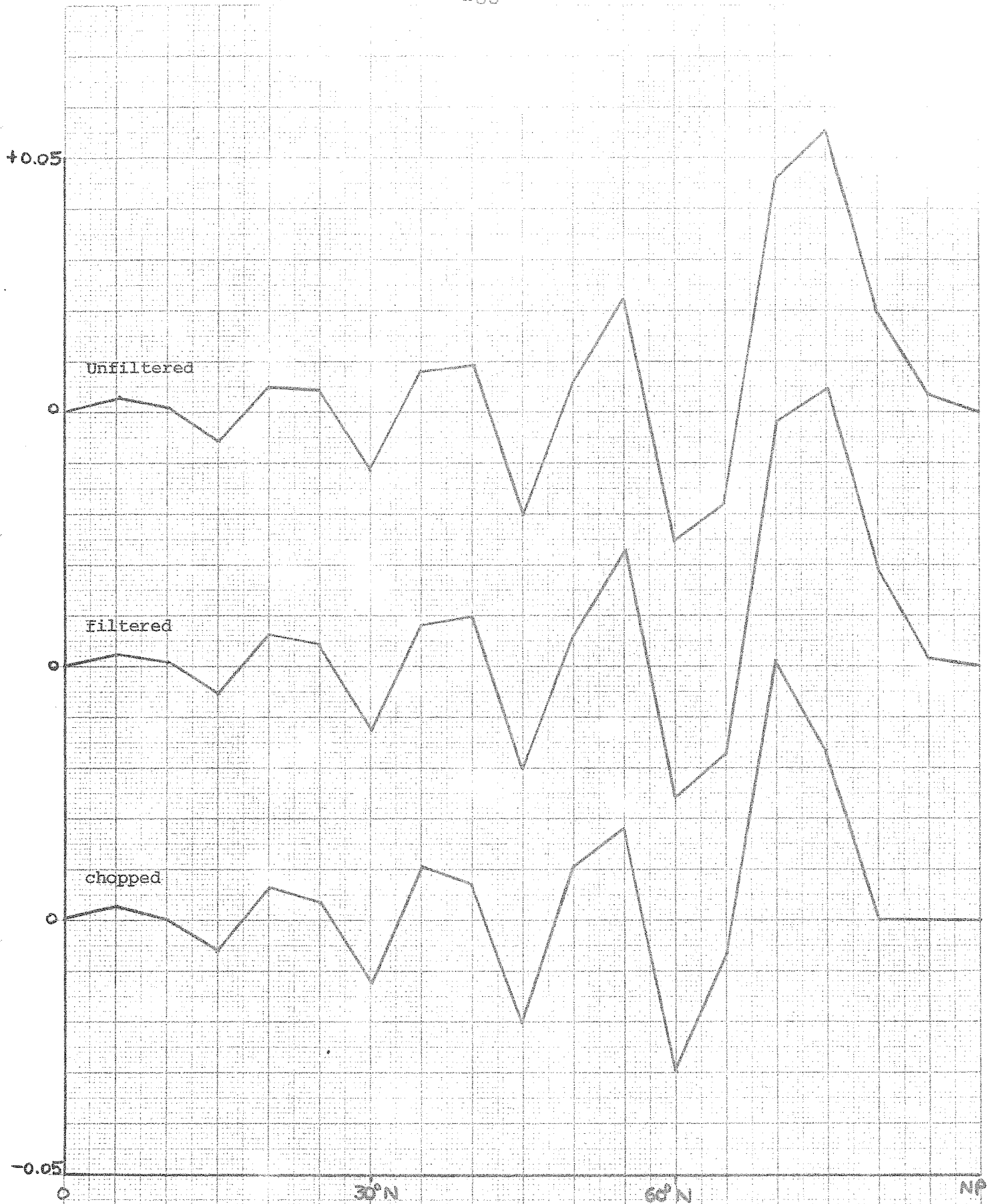


Fig. 10 Rossby mode  $\phi$  profiles:  $k=7$ ,  $l=18$ .

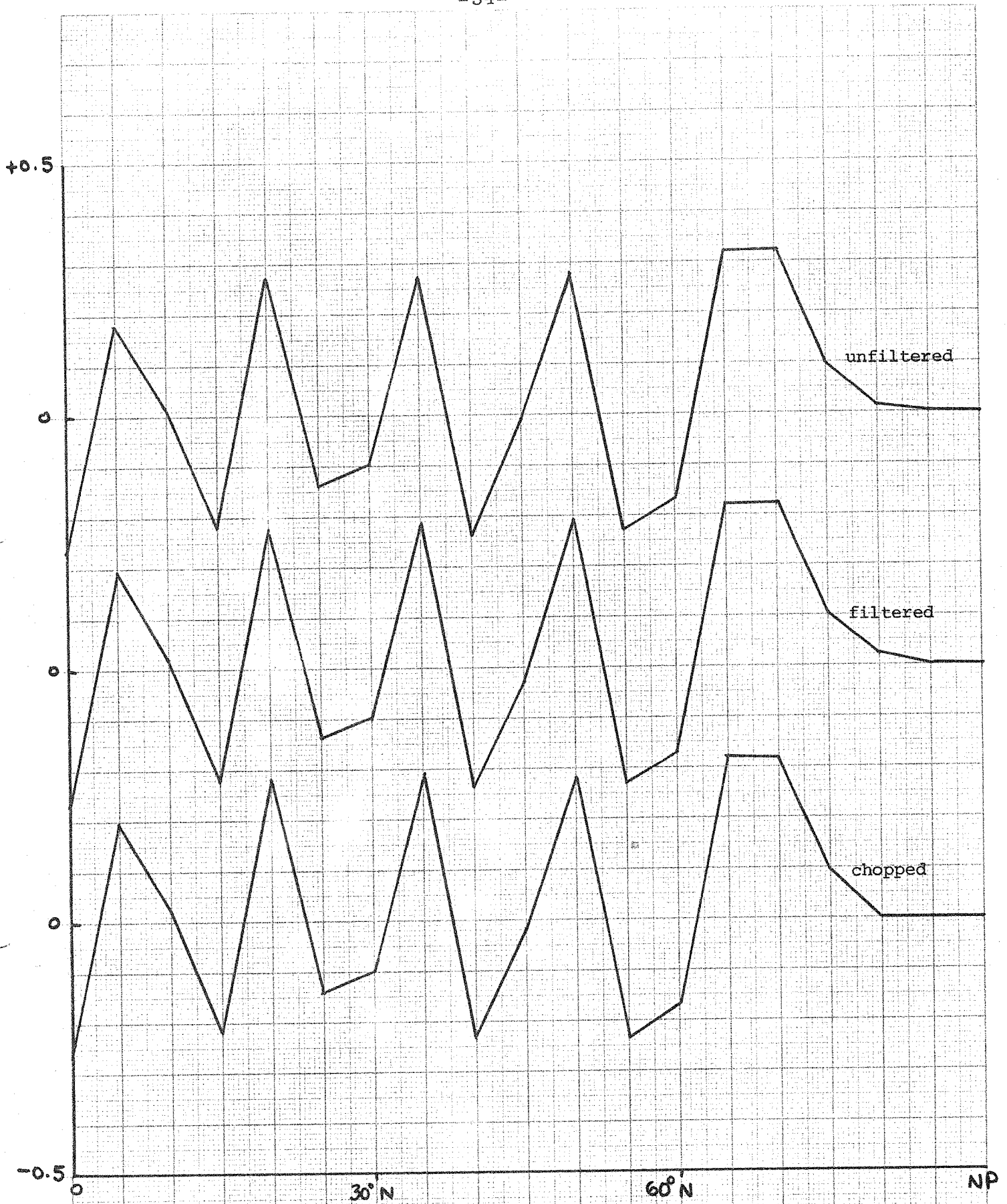


Fig. 11 Westward gravity mode  $\phi$  profiles:  $k=7$ ,  $l=18$ .



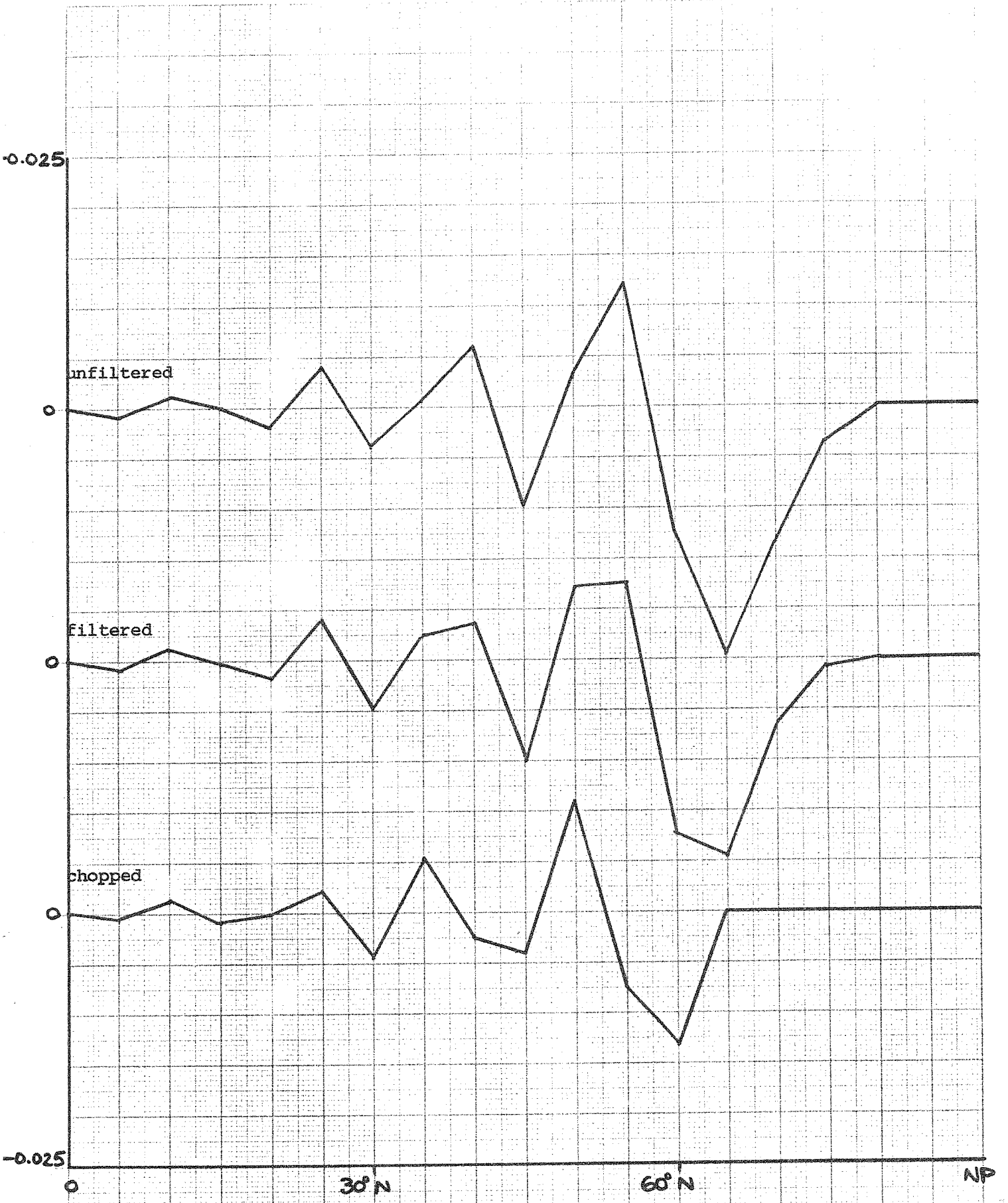


Fig. 12 Rossby mode  $\phi$  profiles:  $k=18$ ,  $l=18$ .

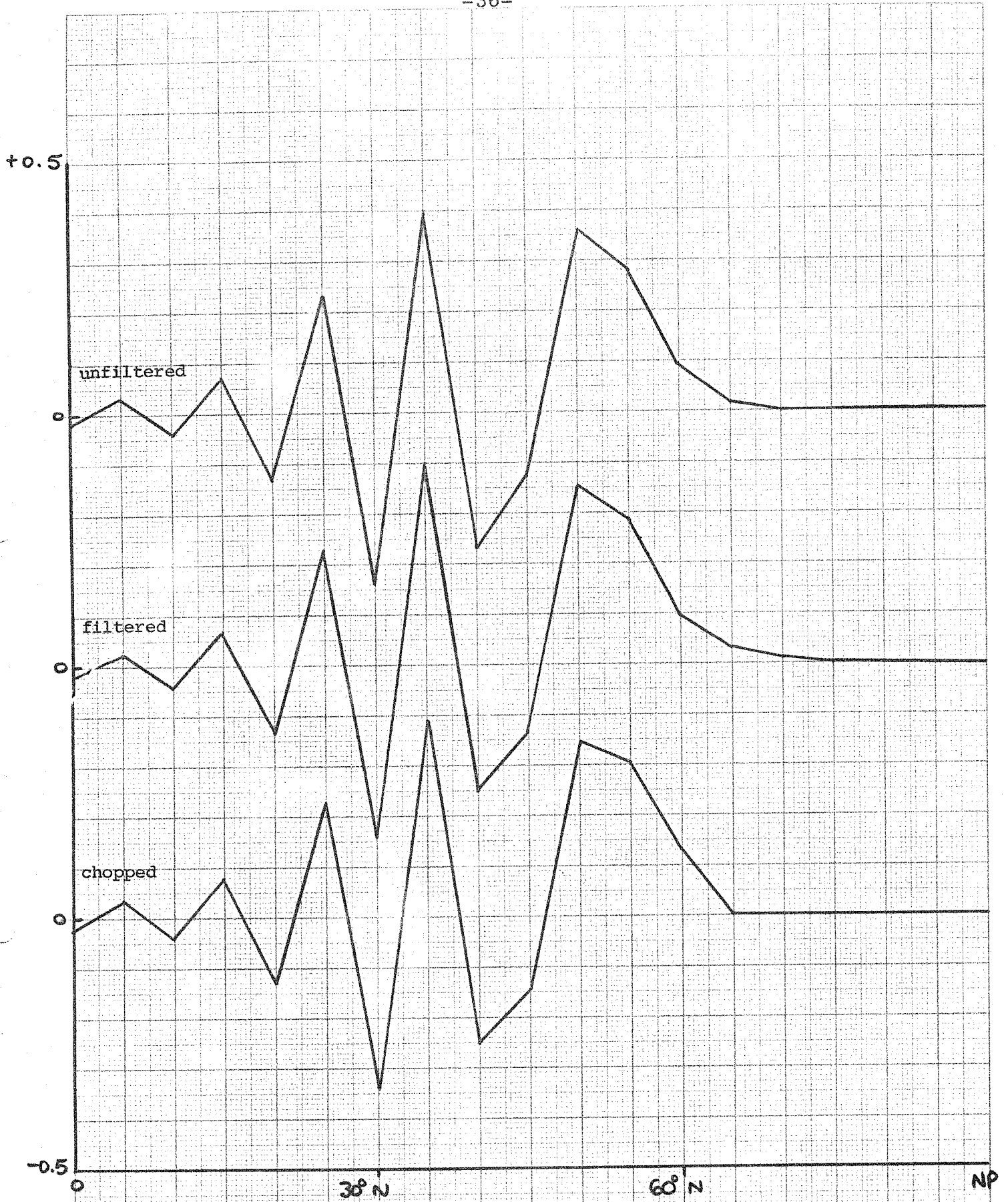


Fig. 13 Westward gravity mode  $\phi$  profiles:  $k=18$ ,  $l=18$ .

APPENDIX: On eastward-moving Rossby modes on a non-staggered grid

The existence of the eastward-moving "bad" Rossby modes in Dickinson and Williamson's model, and their absence in the ECMWF model, can be explained by considering the Rossby wave equation on a beta-plane.

In the continuous case, the linearized equations are

$$\frac{\partial u}{\partial t} - fv + \frac{\partial \phi}{\partial x} = 0 \quad (31)$$

$$\frac{\partial v}{\partial t} + fu + \frac{\partial \phi}{\partial y} = 0 \quad (32)$$

$$\frac{\partial}{\partial x}(32) - \frac{\partial}{\partial y}(31) \Rightarrow \frac{\partial}{\partial t} \left( \frac{\partial v}{\partial x} - \frac{\partial u}{\partial y} \right) + fD + \beta v = 0$$

where  $D = \frac{\partial u}{\partial x} + \frac{\partial v}{\partial y}$ . Setting  $D=0$ ,  $u = -\partial\psi/\partial y$ ,  $v = \partial\psi/\partial x$ ,

we obtain

$$\frac{\partial}{\partial t}(\nabla^2\psi) + \beta\frac{\partial\psi}{\partial x} = 0.$$

Inserting a solution of the form  $\psi(x, y, t) = \psi(t)\exp(ikx+ily)$ ,

$$(k^2+l^2)\frac{\partial\psi}{\partial t} = i\beta k\psi \quad (33)$$

$$\therefore \psi(t) = \psi_0 \exp\left(\frac{i\beta kt}{k^2+l^2}\right)$$

So the analytic solutions have positive frequency  $\beta k/(k^2+l^2)$ .

On a staggered grid analogous to that in the ECMWF model, the linearized equations are

$$\frac{\partial u}{\partial t} - f\bar{v}^{xy} + \delta_x\phi = 0 \quad (34)$$

$$\frac{\partial v}{\partial t} + f\bar{u}^{xy} + \delta_y\phi = 0 \quad (35)$$

$$\delta_x(35) - \delta_y(34) \Rightarrow \frac{\partial}{\partial t}(\delta_x v - \delta_y u) + f\bar{D}^{xy} + \beta\bar{v}^{xyy} = 0 \quad (36)$$

where  $D = \delta_x u + \delta_y v$ . Setting  $D=0$ ,  $u = -\delta_y\psi$ ,  $v = \delta_x\psi$ , we obtain

$$\frac{\partial}{\partial t}(\delta_{xx}\psi + \delta_{yy}\psi) + \beta\delta_x\bar{\psi}^{xyy} = 0$$

Inserting a solution  $\psi(x, y, t) = \psi(t)\exp(ikx+ily)$ ,

$$(\bar{k}^2 + \bar{l}^2)\frac{\partial\psi}{\partial t} = i\beta\bar{k}\bar{\psi}^{yy}$$

where  $\bar{k} = \frac{\sin(\frac{1}{2}k\Delta x)}{\frac{1}{2}\Delta x}$ ,  $\bar{l} = \frac{\sin(\frac{1}{2}l\Delta y)}{\frac{1}{2}\Delta y}$ ,  $\bar{k} = \frac{\sin(k\Delta x)}{\Delta x}$ ,

which gives the following analogue of Eq. (33):

$$(\bar{k}^2 + \bar{l}^2) \frac{\partial \psi}{\partial t} = i\beta \bar{k} \cdot \frac{1}{2}(1 + \cos(l\Delta y))\psi.$$

Since  $\frac{1}{2}(1 + \cos(l\Delta y)) \geq 0$  for all  $l$  (with equality only for 2-gridlength waves), there are no solutions on this grid with negative frequencies (i.e. no eastward-moving solutions).

On a non-staggered grid, as in the model of Dickinson and Williamson, the linearized equations are

$$\frac{\partial u}{\partial t} - fv + \delta_x \bar{\phi}^x = 0 \quad (37)$$

$$\frac{\partial v}{\partial t} + fu + \delta_y \bar{\phi}^y = 0 \quad (38)$$

$$\delta_x (38^x) - \delta_y (37^y) \Rightarrow \frac{\partial}{\partial t} (\delta_x \bar{v}^x - \delta_y \bar{u}^y) + fD + \beta \bar{v}^x(2y) = 0 \quad (39)$$

where  $D = \delta_x \bar{u}^x + \delta_y \bar{v}^y$ . Setting  $D=0$ ,  $u = -\delta_y \bar{\psi}^y$ ,  $v = \delta_x \bar{\psi}^x$ ,

we obtain

$$\frac{\partial}{\partial t} (\delta_{xx} \bar{\psi}^{xx} + \delta_{yy} \bar{\psi}^{yy}) + \beta \delta_x \bar{\psi}^x(2y) = 0.$$

Inserting a solution  $\psi(x, y, t) = \psi(t)\exp(ikx + ily)$ ,

$$(\bar{k}^2 + \bar{l}^2) \frac{\partial \psi}{\partial t} = i\beta \bar{k} \bar{\psi}^x(2y)$$

where  $\bar{l} = \frac{\sin(l\Delta y)}{\Delta y}$ , which gives the following analogue of Eq. (33):

$$(\bar{k}^2 + \bar{l}^2) \frac{\partial \psi}{\partial t} = i\beta \bar{k} \cos(l\Delta y)\psi.$$

For values of  $l$  corresponding to wavelengths shorter than  $4\Delta y$ ,  $\cos(l\Delta y) < 0$ , and so the solutions on this grid with short meridional wavelengths will propagate in the wrong direction, i.e. eastwards.

The crucial difference between the analyses on the two grids lies in the meridional averaging of the  $\beta v$  term in the Rossby wave equation - compare Eqs. (36) and (39).

EUROPEAN CENTRE FOR  
MEDIUM RANGE WEATHER  
FORECASTS

Research Department (RD)

Internal Report No. 12

- No. 1 Users Guide for the G.F.D.L. Model  
(November 1976)
- No. 2 The Effect of Replacing Southern Hemispheric  
Analyses by Climatology on Medium Range  
Weather Forecasts  
(January 1977)
- No. 3 Test of a Lateral Boundary Relaxation Scheme  
in a Barotropic Model  
(February 1977)
- No. 4 Parameterisation of the surface fluxes  
(February 1977)
- No. 5 An Improved Algorithm for the Direct Solution of  
Poisson's Equation over Irregular Regions  
(February 1977)
- No. 6 Comparative Extended Range Numerical Integrations  
with the E.C.M.W.F. Global Forecasting Model  
1: The N24, Non-Adiabatic Experiment  
(March 1977)
- No. 7 The E.C.M.W.F. Limited Area Model  
(March 1977)
- No. 8 A Comprehensive Radiation Scheme designed for  
Fast Computation  
(May 1977)
- No. 9 Documentation for the E.C.M.W.F. Grid Point Model  
(May 1977)
- No. 10 Numerical Tests of Parameterisation Schemes at an  
Actual Case of Transformation of Arctic Air  
(June 1977)
- No. 11 Analysis Error Calculations for the FGGE  
(June 1977)
- No. 12 Normal Modes of a Barotropic Version of the  
E.C.M.W.F. Gridpoint Model  
(July 1977)